ICTS INTERNATIONAL CENTRE *for* THEORETICAL SCIENCES
TATA INSTITUTE OF FUNDAMENTAL RESEARCH

ENTROPY, INFORMATION & ORDER IN SOFT MATTER

"Entropy in Self-Assembly"

Francesco Sciortino
Sapienza **Universita' di Roma**

http://www.roma1.infn.it/~sciortif/

SAPIENZA UNIVERSITÀ DI ROMA

COLLDENSE COLLOIDS with DESIGNED RESPONSE

Outline

- Entropy and Order, Ω (Hard-Sphere Crystallization, Onsager Theory, Entropy in the ground state (Networks, Crystal selection).
- Entropy attracts (Depletion Interactions, Safran, DNA functionalized Colloids)
- Self-Assembly
- When energy and entropy compete (DHS, Re-entrant gel)

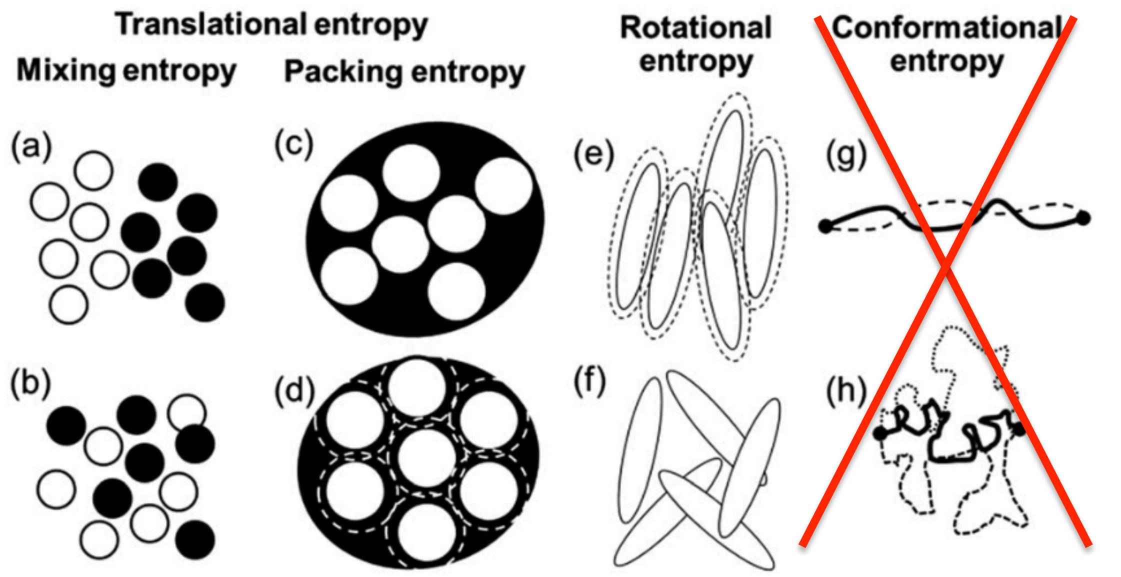

Fig. 1 Examples of different manifestations of entropy. A two-component system in states with segregated components (a) has less entropy than in states where components are spatially intermixed (b). Particles crowding in random configurations (c) could avoid jamming by arranging into orderly patterns (d), thus allowing access to more free volume around each particle (dashed circles). Rod-like particles have more rotational entropy if allowed to have uncorrelated axial orientations (f), but may align and lose orientational entropy if this is compensated by gains in packing entropy (e). Whole polymer chains typically have negligible translational or rotational entropy but have significant conformational entropy; chains lose conformational entropy when forced to have too large end-to-end distances (g) as this reduces the number of conformations accessible when less constrained (h).

Cite this: *Soft Matter*, 2014, 10, 8388

Engineering entropy in soft matter: the bad, the ugly and the good

Fernando A. Escobedo*

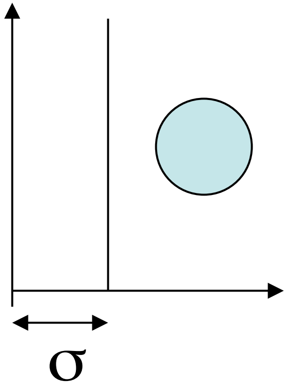

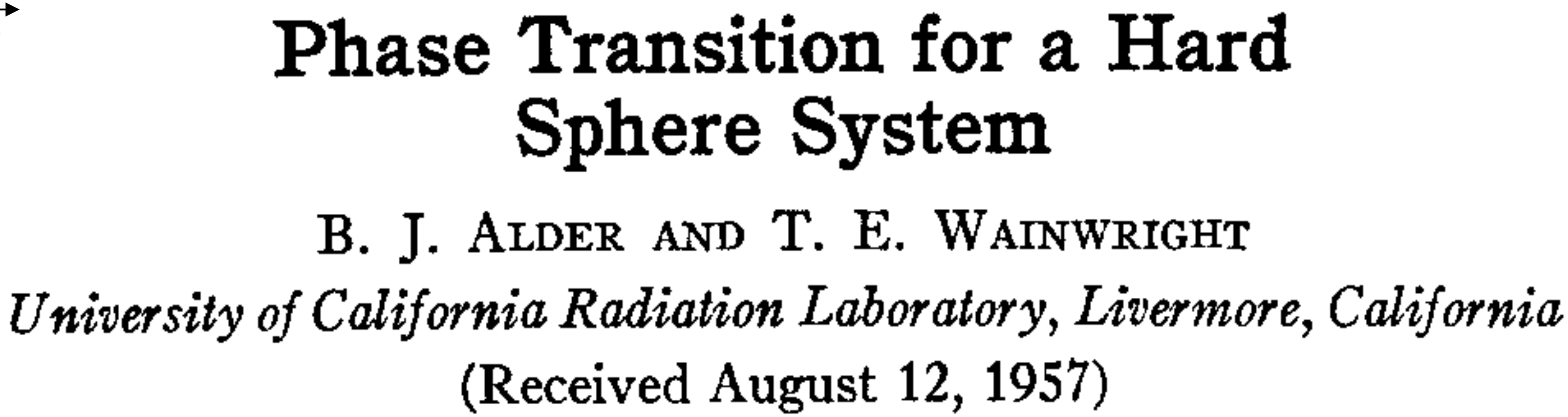

Phase Transition for a Hard Sphere System

B. J. ALDER AND T. E. WAINWRIGHT
University of California Radiation Laboratory, Livermore, California

(Received August 12, 1957)

J. Chem. Phys. 27, 1208 (1957)

Which one is more disordered ?

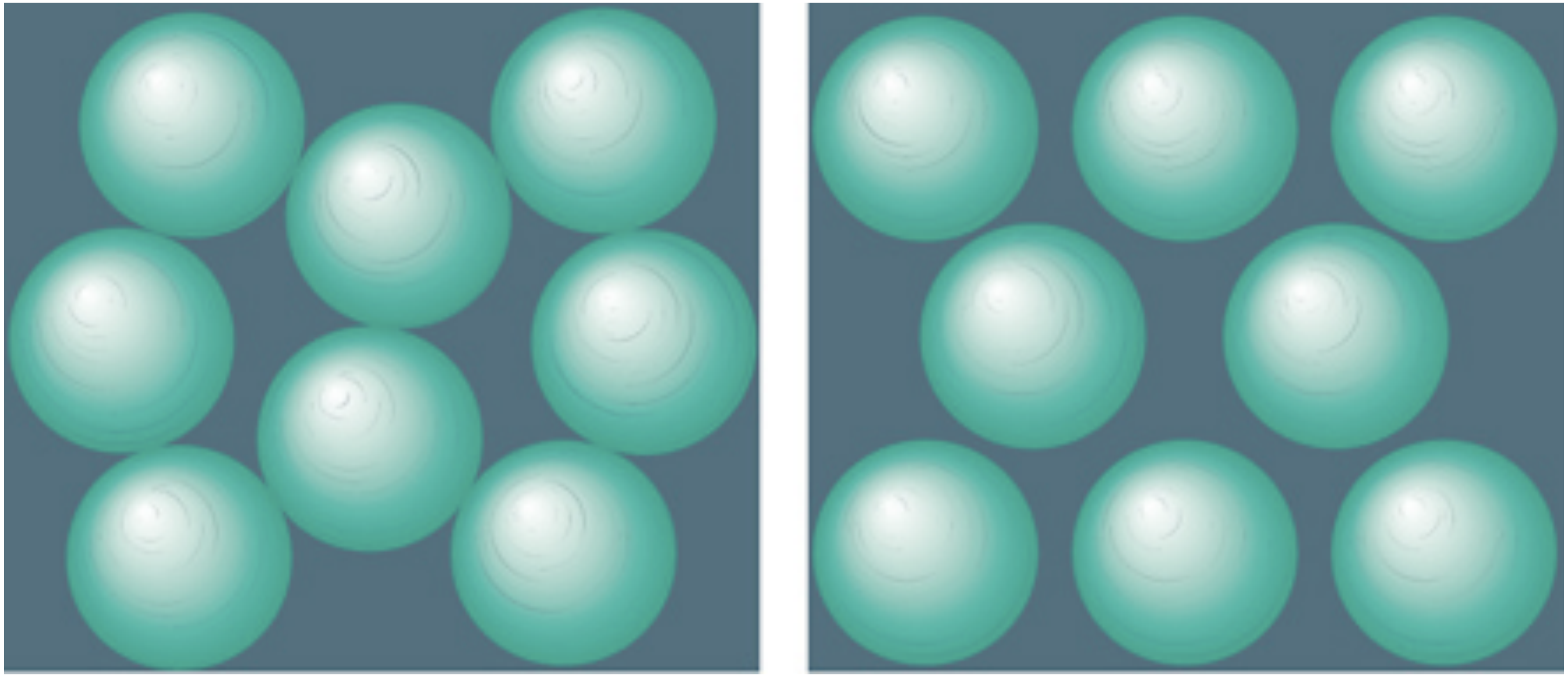

Hard Spheres (HS)

Equilibrium properties

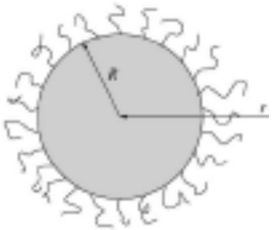

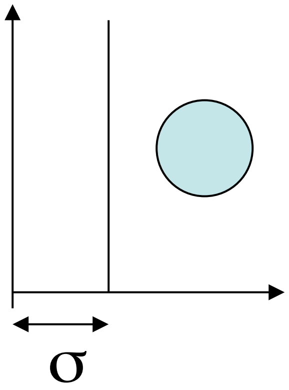

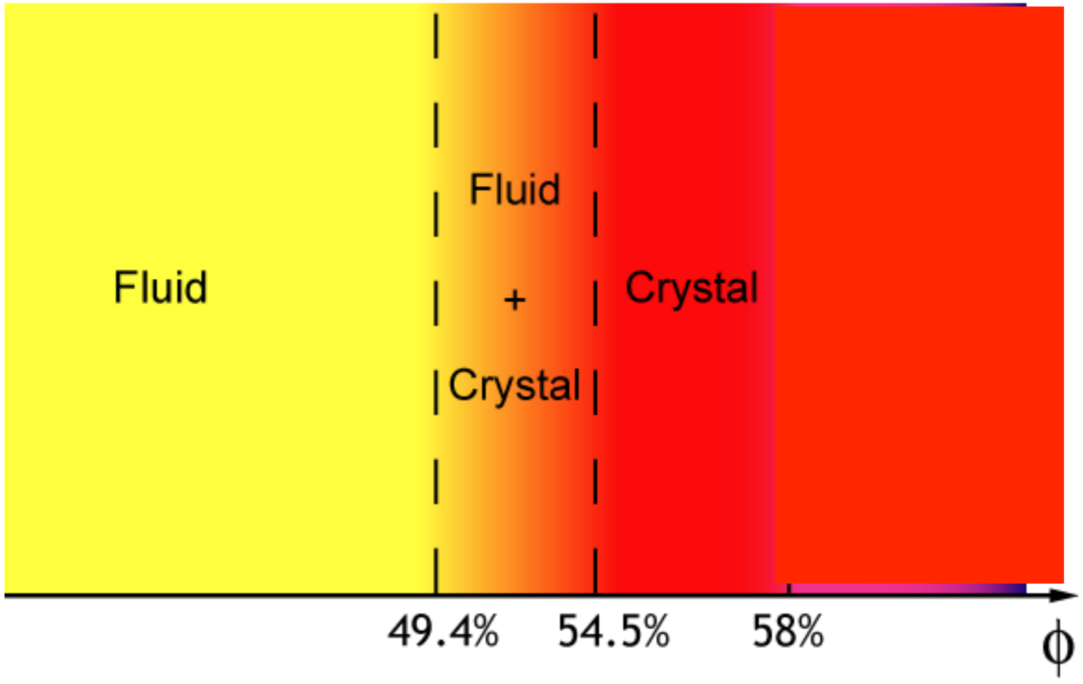

- **Hard spheres present a fluid–solid phase separation due to entropic effects**

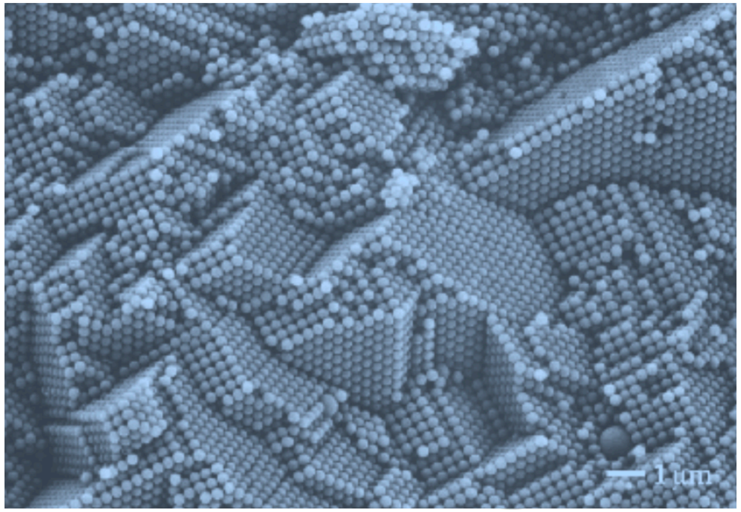

Sterically stabilized PMMA particles (polydispersity 5-10 %)

Courtesy P. Pusey

Entropy in hard-spheres fluid

At constant V, we need to maximize the entropy

1) "Configurational" entropy (topological entropy)
2) Translational (Vibrational) Entropy (cage entropy)

A proxy to translational Entropy...

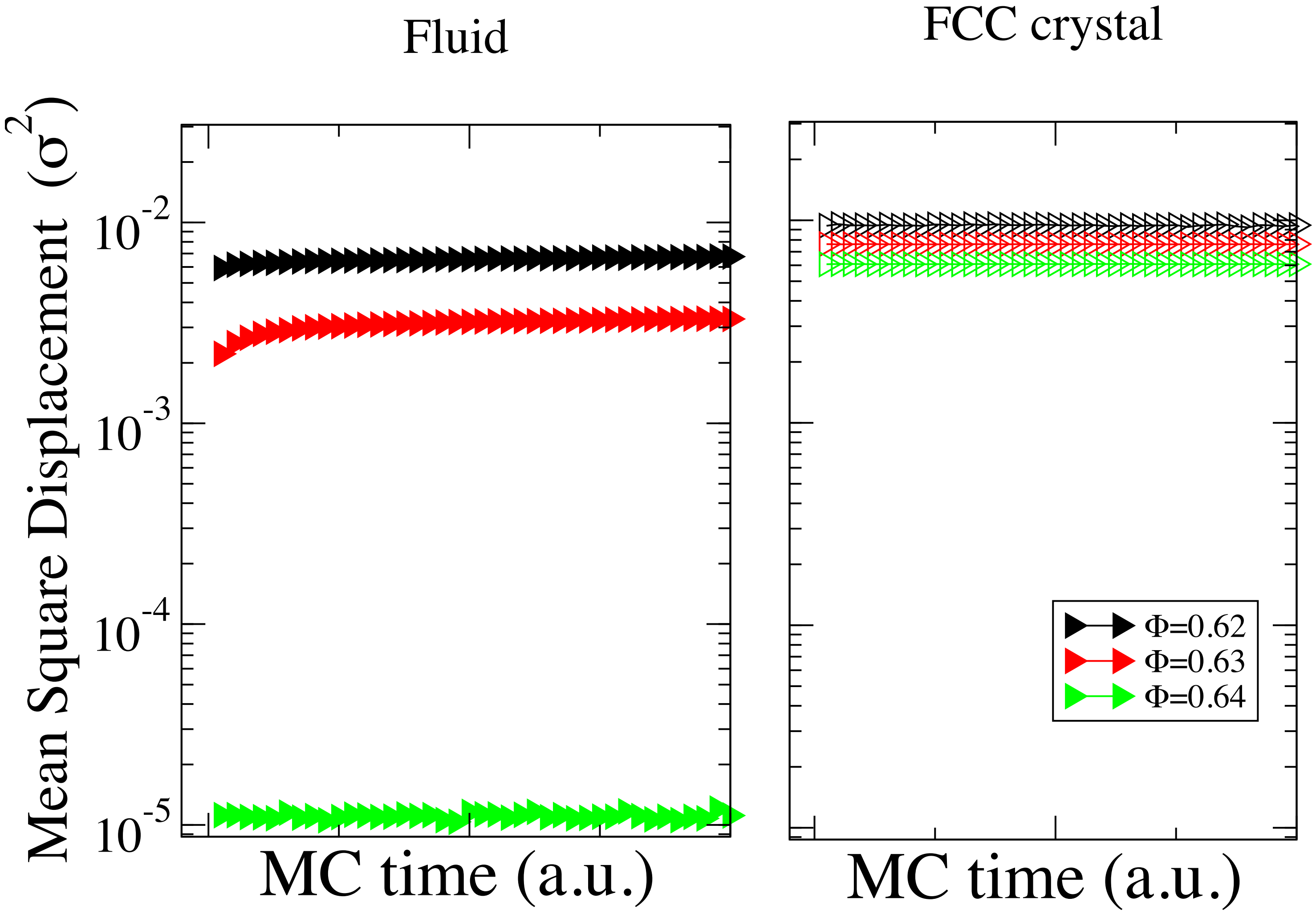

$$\mathrm{MSD}=|\mathbf{r}_i(t)-\mathbf{r}_i(0)|^2$$

SAPIENZA
UNIVERSITÀ DI ROMA

COLLDENSE
COLLOIDS with DESIGNED RESPONSE

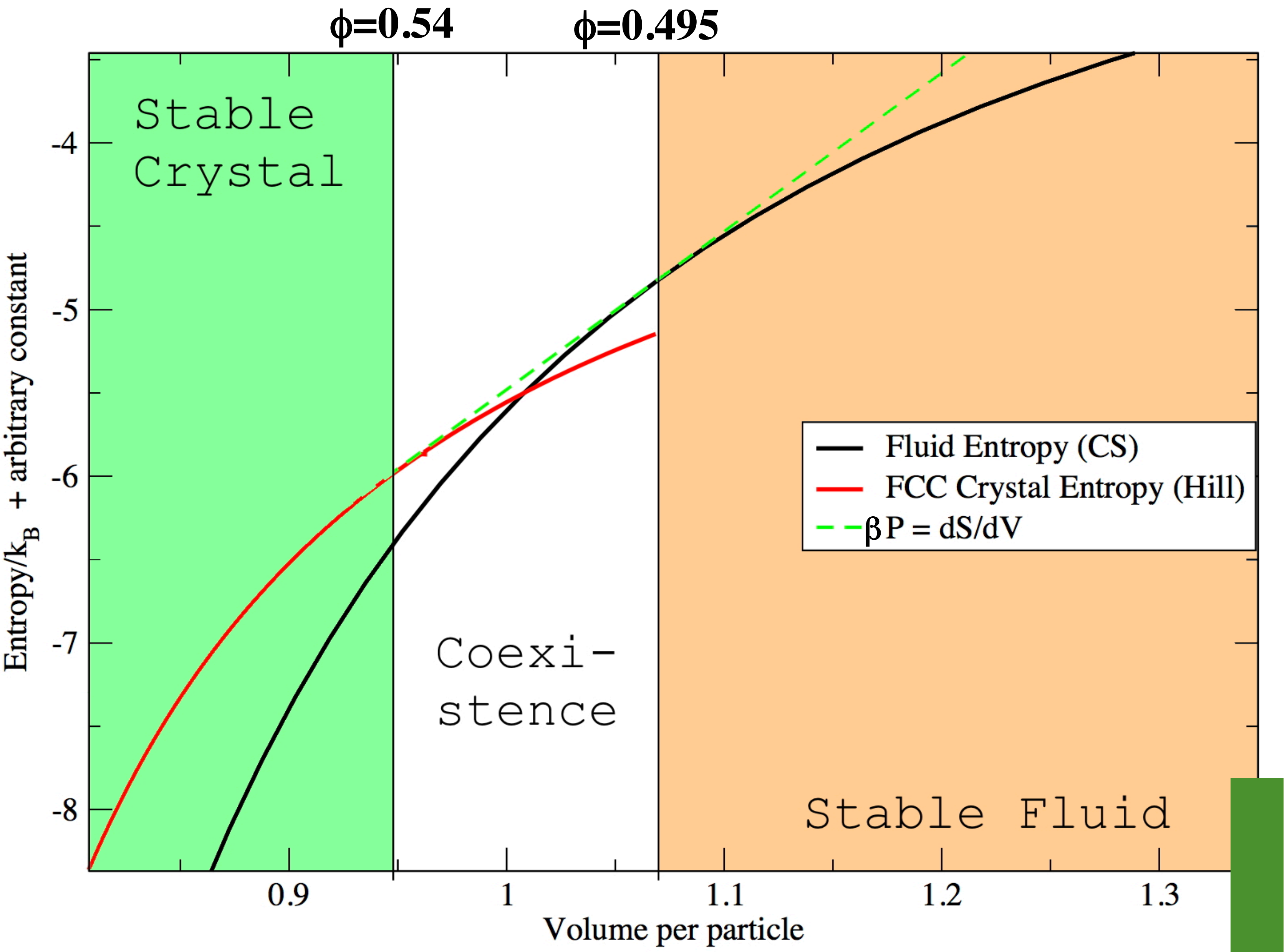
φ=0.54
φ=0.495
Stable Crystal
Coexi-stence
Stable Fluid
Fluid Entropy (CS)
FCC Crystal Entropy (Hill)
βP = dS/dV
Entropy/k_B + arbitrary constant
-4
-5
-6
-7
-8
0.9
1
1.1
1.2
1.3
Volume per particle

Orientational Entropy

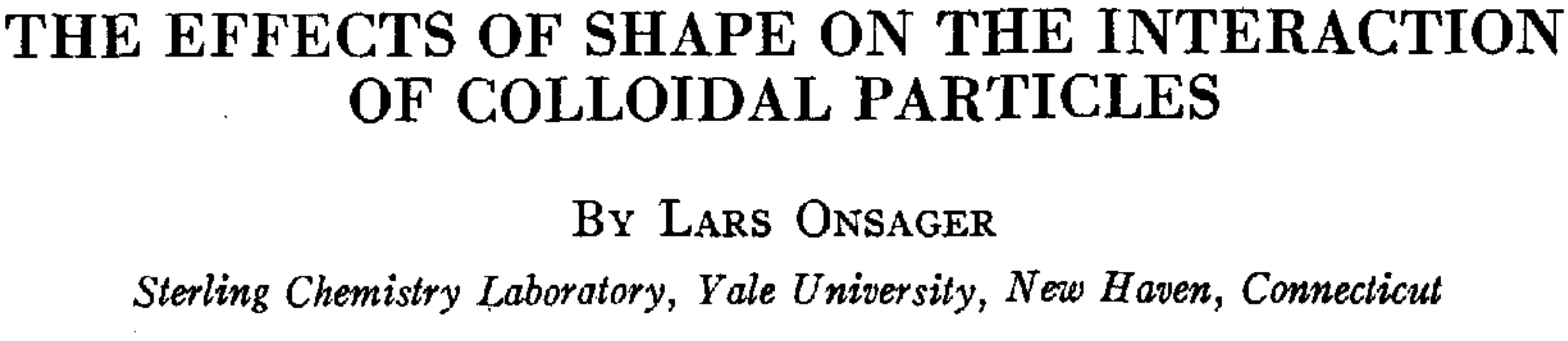

THE EFFECTS OF SHAPE ON THE INTERACTION OF COLLOIDAL PARTICLES

By Lars Onsager

Sterling Chemistry Laboratory, Yale University, New Haven, Connecticut

ANNALS NEW YORK ACADEMY OF SCIENCES 1949

Isotropic-Nematic Transition (Onsager Theory)

Isotropic

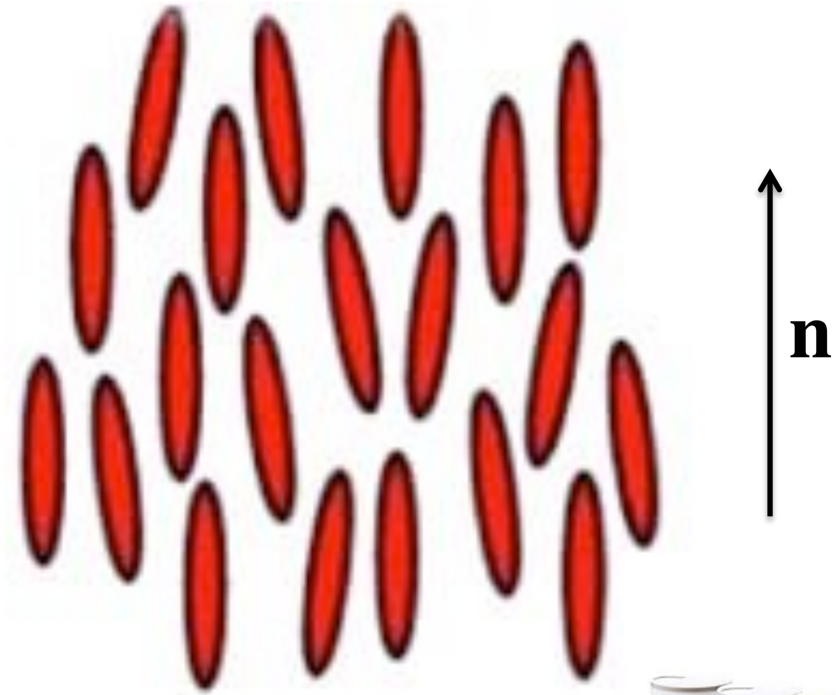

Nematic

Let's assume that particles can be considered distinct according to the orientation of their principal axis $\mathbf{a}$. Then, the partition function of an ideal gas of these particles can be written as

$$Z = \prod_i \frac{1}{\Delta N_i!}\left[\frac{\int\int d\mathbf{r}d\Omega}{4\pi}\right]^{\Delta N_i}$$

and the corresponding free-energy (defining $\Delta\Omega_i = \sin\theta_i \Delta\theta_i \Delta\phi_i$) as

$$-\frac{S}{k_B} = \sum_i \Delta N_i \left[1 + \ln\left(\frac{V\Delta\Omega_i}{4\pi\Delta N_i}\right)\right]$$

If we add the virial contribution, thus going beyond the ideal gas approximation, one obtains

$$-\frac{S}{k_B} = \sum_i \Delta N_i \left[1 + \ln\left(\frac{V\Delta\Omega_i}{4\pi\Delta N_i}\right)\right] + \frac{1}{2V}\sum_{i,j}\beta(\mathbf{a_i},\mathbf{a_j})\Delta N_i \Delta N_j$$

where $\beta(\mathbf{a_i},\mathbf{a_j})$ is the virial coefficient (the excluded volume) between two particles oriented as $\mathbf{a_i}$ and $\mathbf{a_j}$

For cylinders of length l and diameter d, indicating with γ the angle between $\mathbf{a_i}$ and $\mathbf{a_j}$

$$-\beta(\gamma) = \frac{\pi}{2}d^3\sin\gamma + \frac{\pi}{2}l^2 d + \frac{\pi}{2}ld^2|\cos\gamma| + 2ld^2E(\sin\gamma) + 2l^2d|\sin\gamma|$$

where

$$E(\sin\gamma) = \int_0^{\frac{\pi}{2}}(1-\sin^2\gamma\sin^2\phi)^{1/2}d\phi$$

If $L \gg d$,

$$\beta(\gamma) = -2l^2d|\sin\gamma|$$

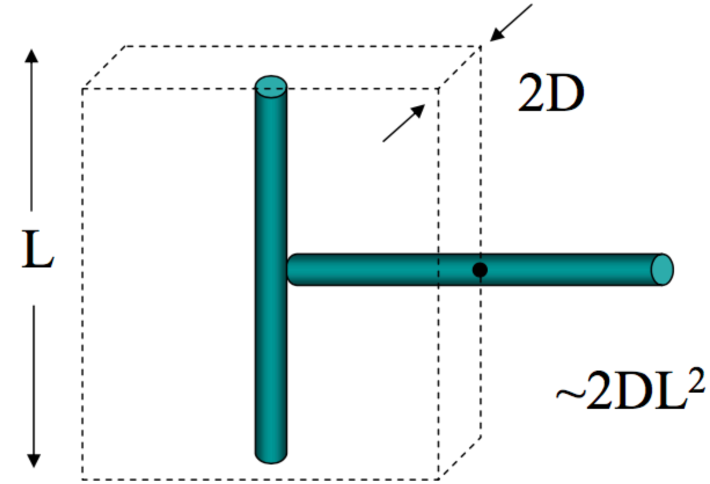

γ=90

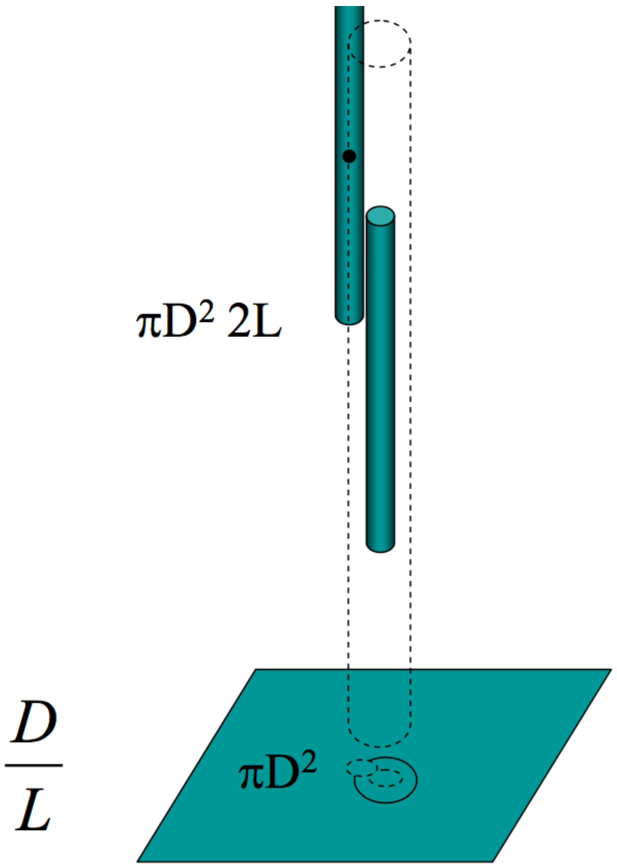

γ=0

significant reduction of sampled phase space !!!!

It is convenient to normalize ΔN_i by N, such that $f(\mathbf{a_i})$ becomes the probability of observing a particle oriented in the solid angle $\Delta\Omega_i$. In this way

$$\Delta N_i = N f(\mathbf{a_i})\Delta\Omega_i \quad \text{with} \quad \int f(\mathbf{a_i})d\Omega = 1$$

In the isotropic case, all orientations are equally probable and $f(\mathbf{a_i}) = \frac{1}{4\pi}$.

For the nematic case, we do not know a priori $f(\mathbf{a})$. Onsager postulated a functional form for $f(\mathbf{a})$ based on an additional parameter α that was then fixed by maximizing the nematic entropy. His choice was (calling θ the angle between $\mathbf{a}$ and the nematic direction)

$$f(\theta) = \left(\frac{\alpha}{4\pi\sinh\alpha}\right)\cosh(\alpha\cos\theta)$$

Onsager shows how to calculate $\frac{1}{2V}\int\int\beta(\gamma)\frac{N^2}{(4\pi)^2}d\Omega d\Omega'$ when $\alpha \gg 1$ as well as how to maximize S to evaluate α.

Now let's compare the isotropic and the nematic case. First, let's highlight the orientational entropy:

$$-\frac{S}{k_B} = \sum_i \Delta N_i\left[1 + \ln\left(\frac{V\Delta\Omega_i}{4\pi\Delta N_i}\right)\right] =$$

$$\int N f(\mathbf{a_i})\Delta\Omega_i\left[1 + \ln\left(\frac{V}{4\pi N f(\mathbf{a_i})}\right)\right] = N\left[1 + \ln\left(\frac{V}{N}\right)\right] - N\int f(\mathbf{a_i})\ln\left(4\pi f(\mathbf{a_i})\right)$$

The last contribution is the orientational entropy.

$\alpha=10$, $f(\theta)$

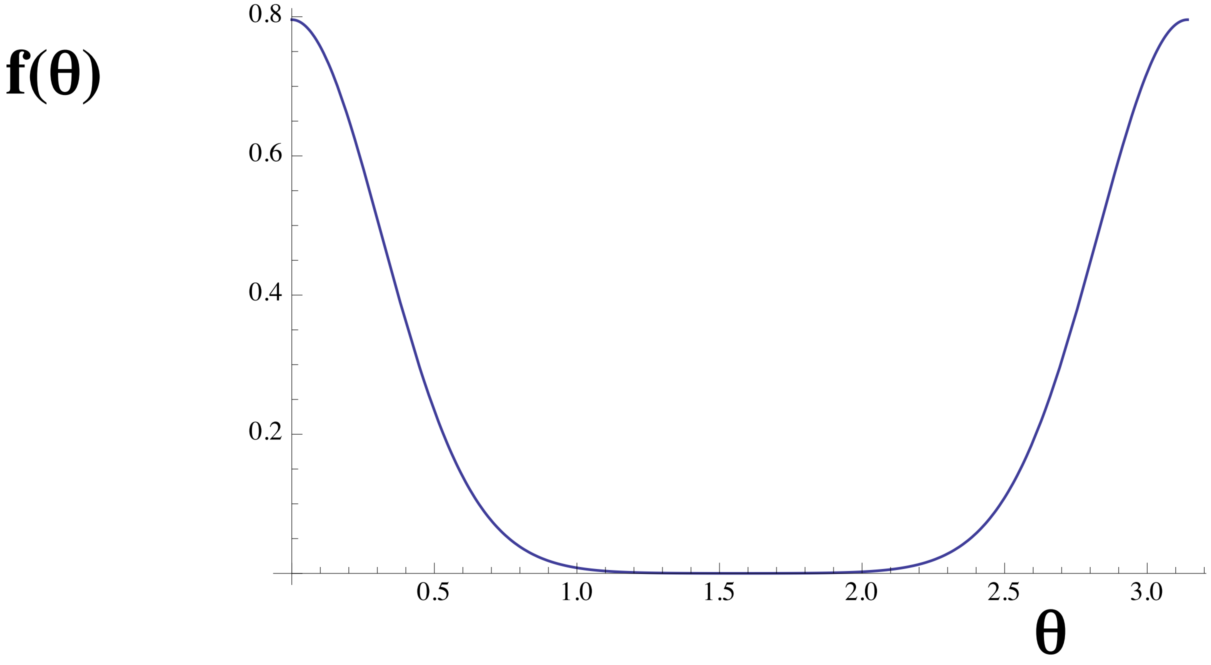

In the case of the nematic, there is an additional contribution equal to

$$\int f(\mathbf{a_i}) \ln\left(4\pi f(\mathbf{a_i})\right) = \log\alpha - 1 + \frac{2}{3\alpha}$$

This contribution diverges to minus infinity with growing α, as expected by localization in classical physics.

Let's see now β_2. For the isotropic case, always in the limit $L \gg d$, (using $\int_0^\pi \sin^2\gamma d\gamma = \pi/2$ and $\int_0^{2\pi} d\phi = 2\pi$)

$$\sum_{i,j} \beta(\mathbf{a_i},\mathbf{a_j})\Delta N_i \Delta N_j = 2l^2 d \int\int \beta(\gamma)\frac{N^2}{(4\pi)^2} d\Omega d\Omega' = N^2 \frac{1}{4\pi}\int \beta(\gamma) sin\gamma d\gamma d\phi = -2l^2 d N^2 \frac{\pi}{4}$$

The corresponding expression for the nematic case (see Onsager article)

$$N^2 \int \beta(\gamma) f(\Omega) f(\Omega') sin\gamma d\gamma d\phi \approx -2l^2 d N^2 9\sqrt{2}\alpha^{-1/2}\pi^{-3/2}$$

which approaches zero for large values of α.

--

Dashed ➔ Isotropic Full ➔ Nematic

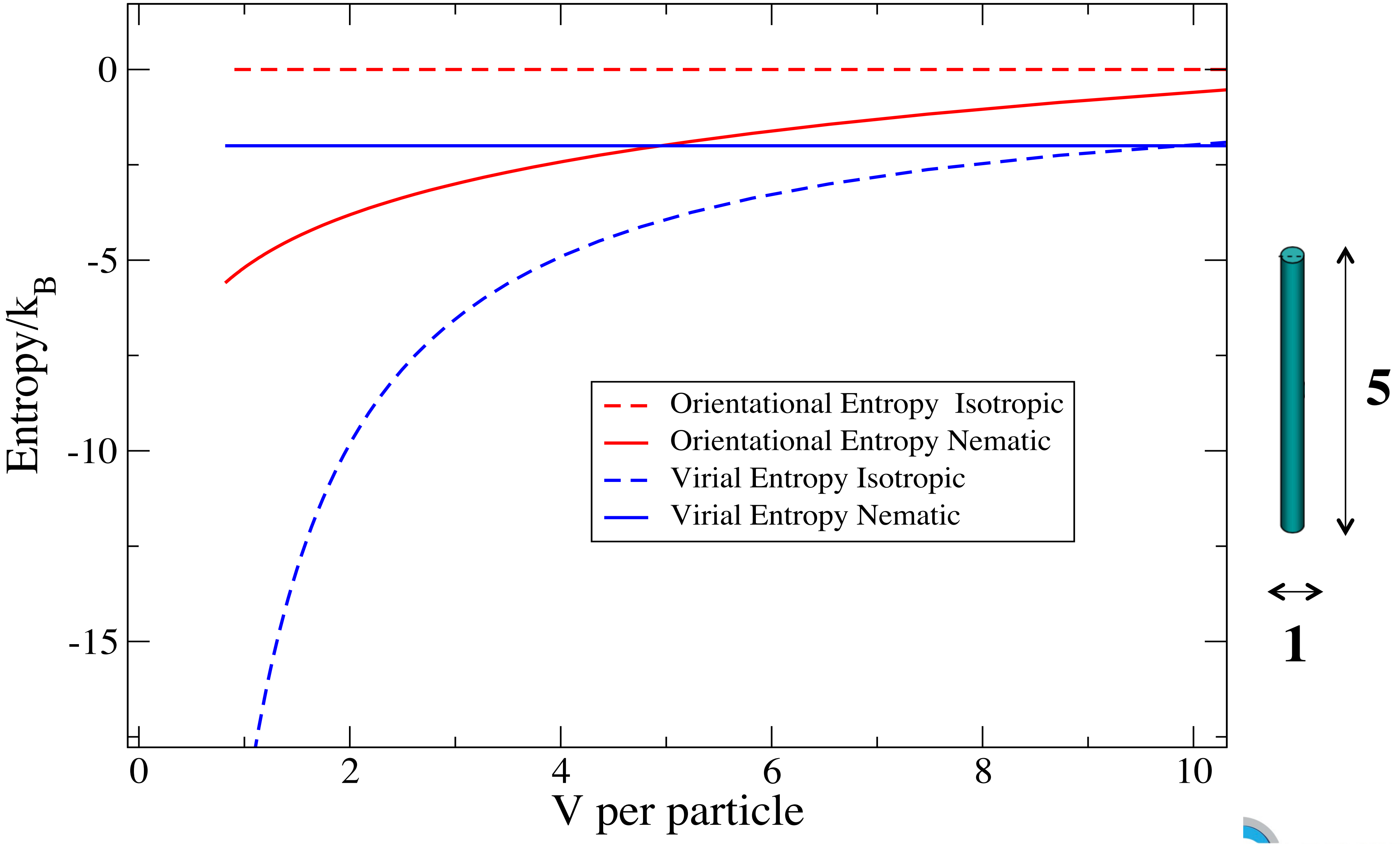

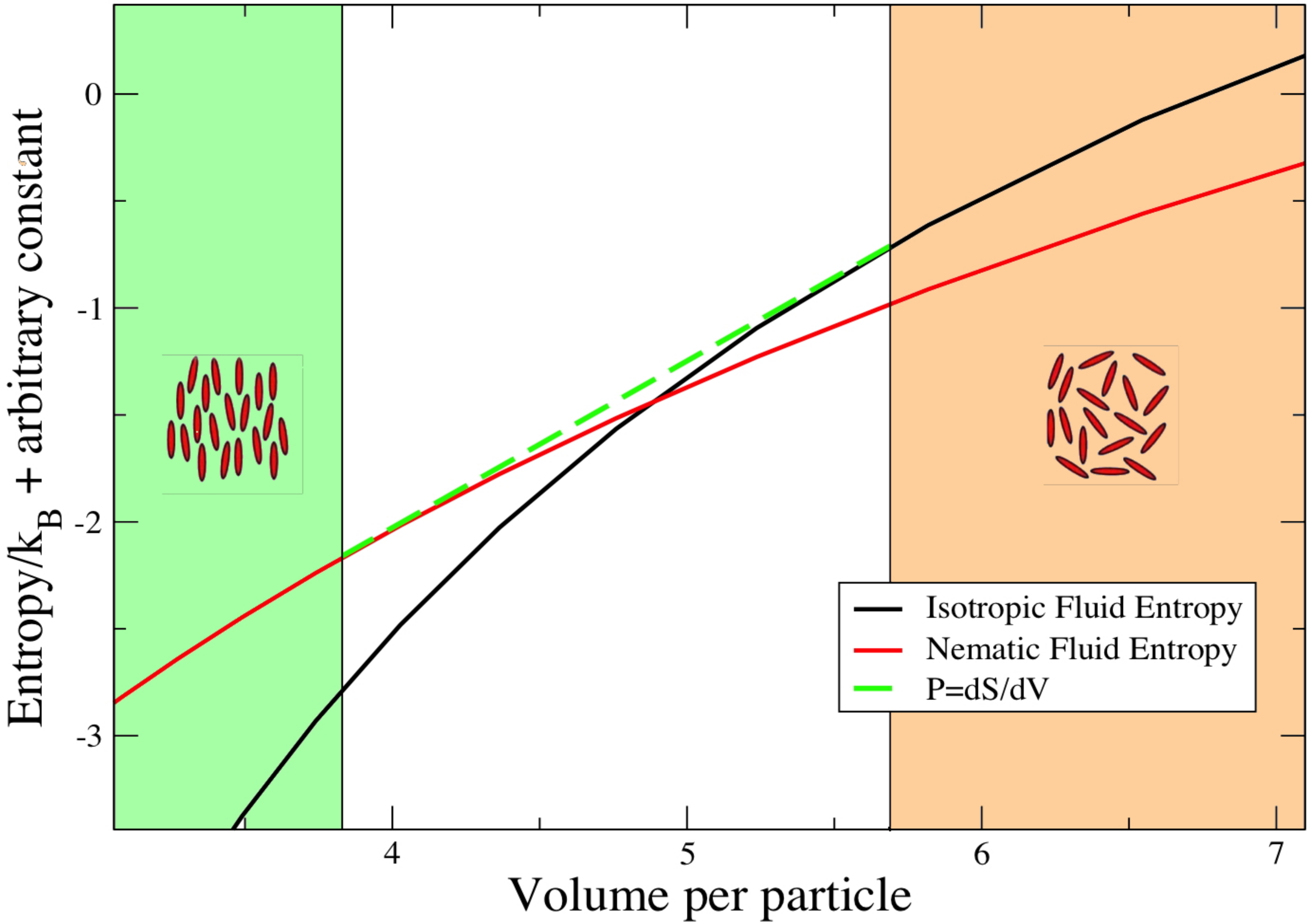
Entropy/k$_B$ + arbitrary constant
0
-1
-2
-3
4
5
6
7
Volume per particle
Isotropic Fluid Entropy
Nematic Fluid Entropy
P=dS/dV

Nematic to...

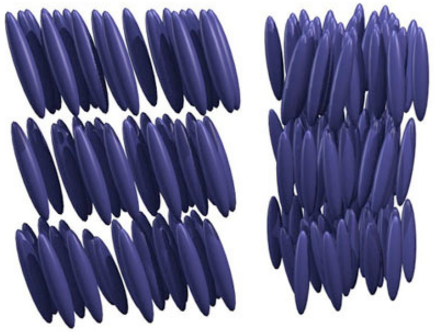

Smectic

Chiral-Cholesteric

Discotic

Biaxial Nematic

Twist-bend Nematic

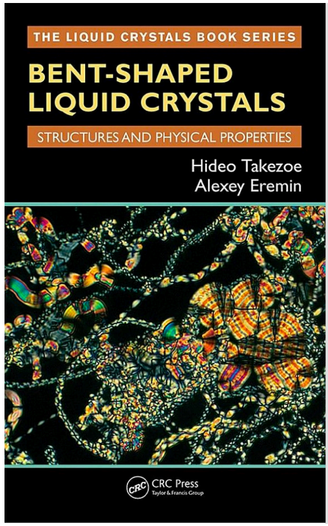

THE LIQUID CRYSTALS BOOK SERIES

BENT-SHAPED
LIQUID CRYSTALS

STRUCTURES AND PHYSICAL PROPERTIES

Hideo Takezoe
Alexey Eremin

CRC Press
Taylor & Francis Group

How do we calculate the fluid entropy numerically

$$F = U - TS \qquad dF = dU - TdS - SdT = dU - dQ - SdT = -PdV - SdT$$

Along an isotherm (which does not cross a first-order line)

$$dF = -PdV \quad F(V,T) = F_{ideal-gas}(V,T) - \int_{\infty}^{V} P_{ex}(V')dV' = F_{ideal-gas}(V,T) - \int_{0}^{N/V} \frac{P_{ex}(\rho)}{\rho^2} d\rho$$

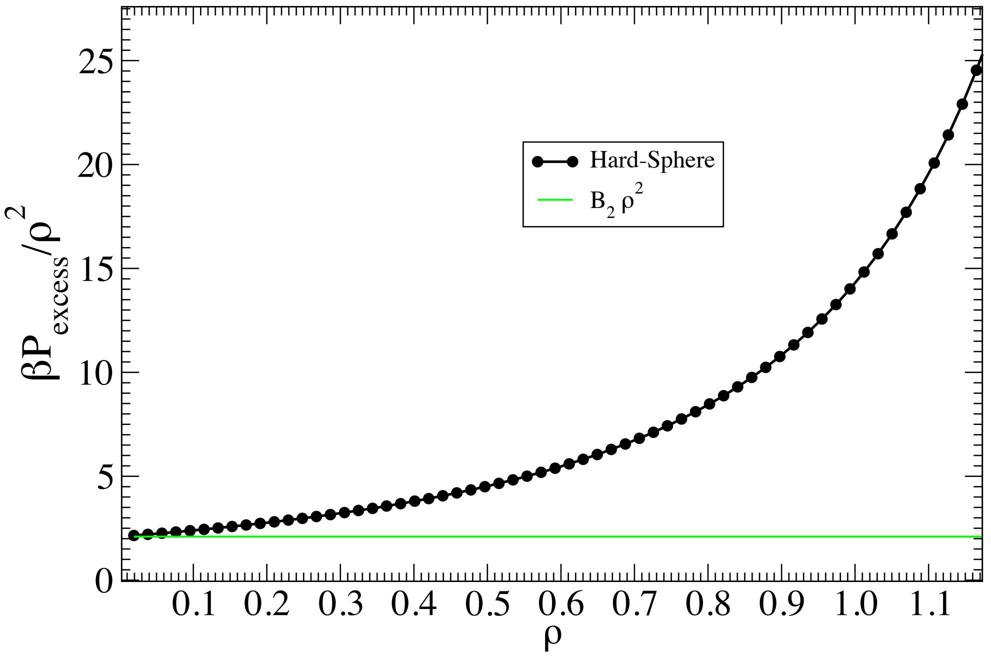

How do we calculate the crystal entropy (free-energy) numerically

$$H(\lambda) = (1-\lambda)H_E + \lambda H_{model}$$

$$H(0) = H_E \qquad H(1) = H_{model}$$

$$\beta F(\lambda) = -\ln \int e^{-\beta H(\lambda)} d\mathbf{r}^N \quad \frac{\partial \beta F(\lambda)}{\partial \lambda} = \frac{1}{\int e^{-\beta H(\lambda)} d\mathbf{r}^N} \frac{\partial}{\partial \lambda} \int e^{-\beta H(\lambda)} d\mathbf{r}^N =$$

$$= \frac{1}{\int e^{-\beta H(\lambda)} d\mathbf{r}^N} \int (H_{model} - H_E) e^{-\beta H(\lambda)} d\mathbf{r}^N = < H_{model} - H_E >_\lambda$$

Then

$$\beta F(1) = \beta F(0) + \int_0^1 d\lambda \frac{\partial \beta F(\lambda)}{\partial \lambda} = \beta F(0) + \int_0^1 < H_{model} - H_E >_\lambda d\lambda$$

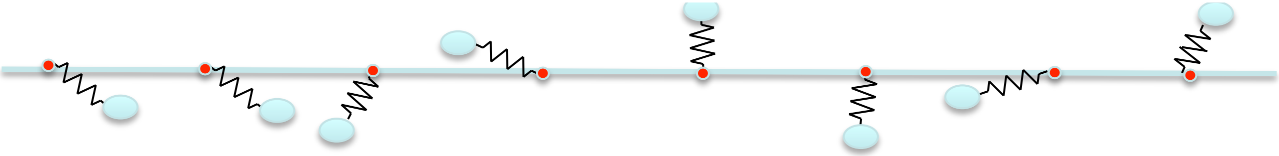

Entropy and flexibility (translation+rotation)

(networks··· limited valence··· patchy particles)

if the liquid reaches a fully bonded state, then it has the same energy than the crystal !

Example of patchy particles

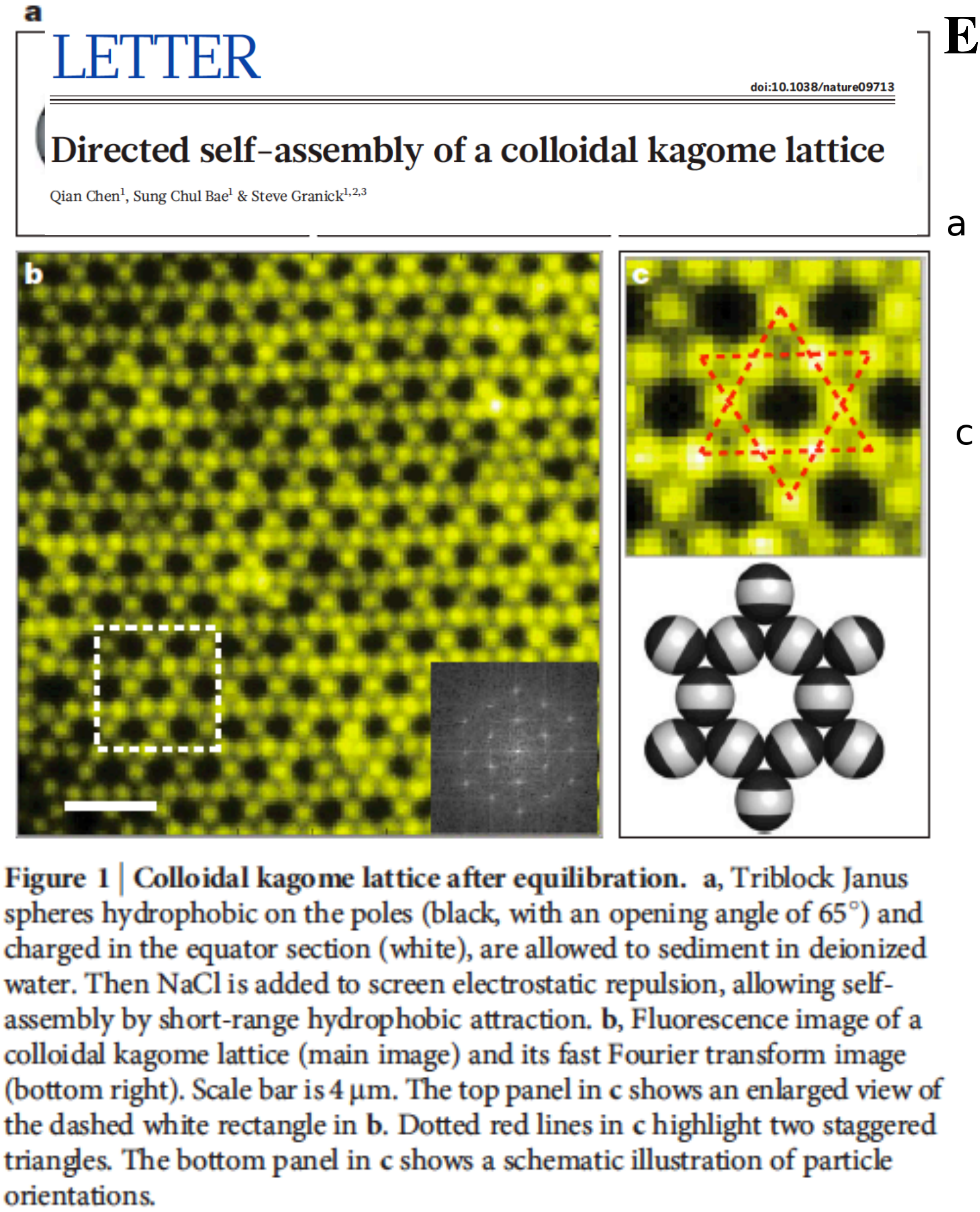

LETTER

doi:10.1038/nature09713

Directed self-assembly of a colloidal kagome lattice

Qian Chen[1], Sung Chul Bae[1] & Steve Granick[1,2,3]

Figure 1 | Colloidal kagome lattice after equilibration. a, Triblock Janus spheres hydrophobic on the poles (black, with an opening angle of 65°) and charged in the equator section (white), are allowed to sediment in deionized water. Then NaCl is added to screen electrostatic repulsion, allowing self-assembly by short-range hydrophobic attraction. **b,** Fluorescence image of a colloidal kagome lattice (main image) and its fast Fourier transform image (bottom right). Scale bar is 4 μm. The top panel in **c** shows an enlarged view of the dashed white rectangle in **b**. Dotted red lines in **c** highlight two staggered triangles. The bottom panel in **c** shows a schematic illustration of particle orientations.

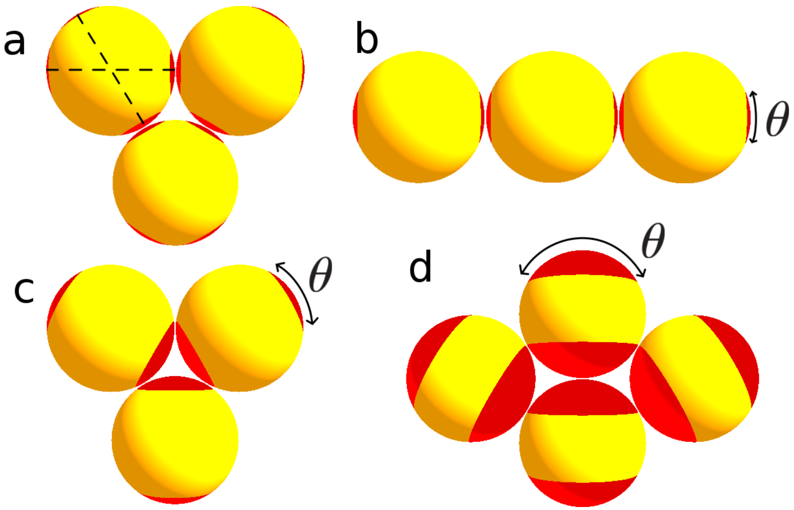

DNA constructs: Limited-valence patchy particles

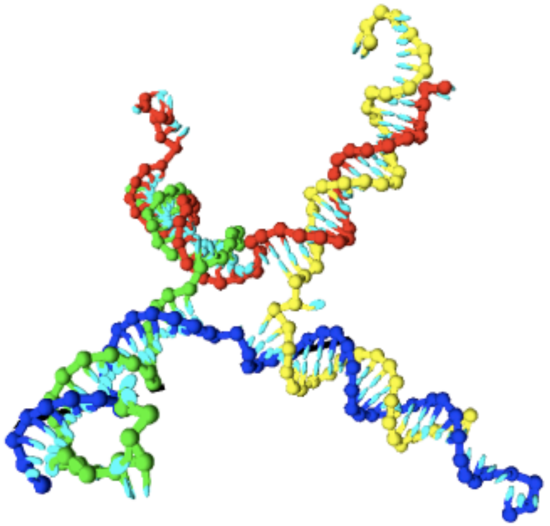

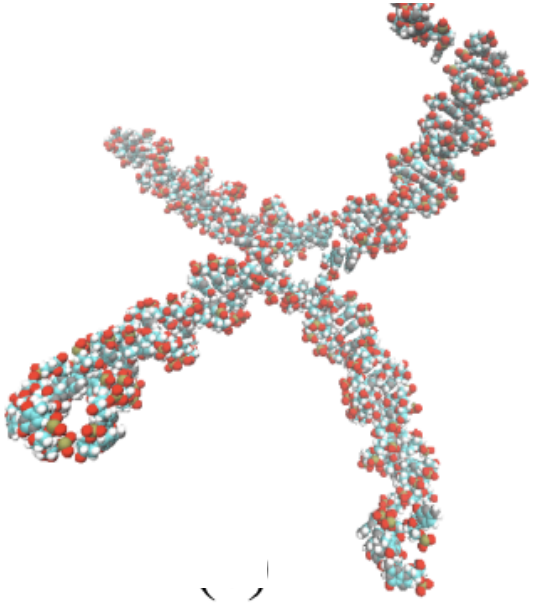

DNA-coated patchy colloids

J. Phys.: Condens. Matter **25** (2013) 193101 Topical Review

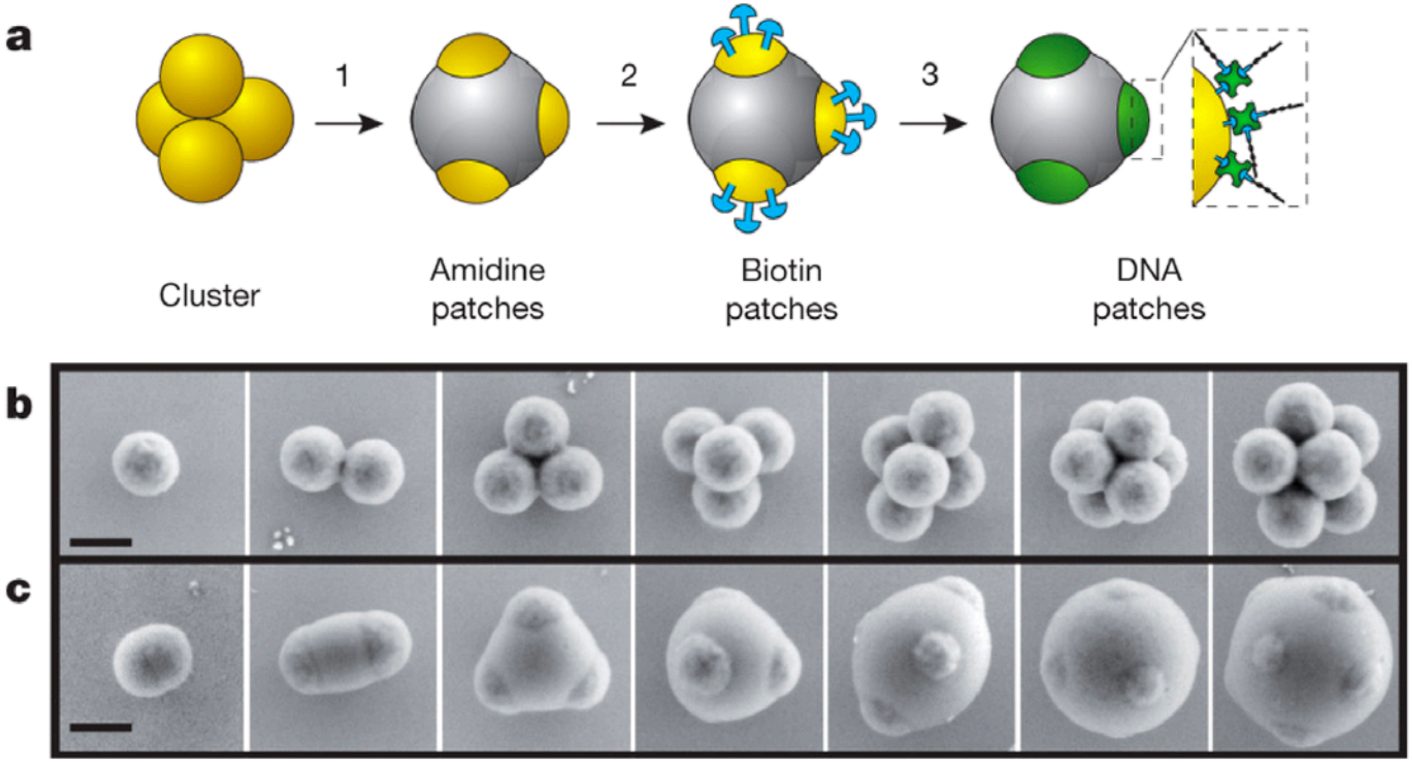

Figure 9. (a) Schematic diagram of seeded polymerization on tetrahedral colloidal clusters. (b) and (c) SEM image of colloidal clusters ($N = 1$–7) and their patchy particles. (Reprinted with permission from [10]. Copyright 2012 Nature Publishing Group.)

Gi-Ra Yi, David J Pine and Stefano Sacanna

All particles are bonded with four neighbours

There are loops of different length

Particles “vibrate” around equilibrium positions.

How about (low density) crystals ?

Entropy decides the most stable phase (exactly as in HS!)

Competition between:

- **Number of microstates accessed at fixed bonding" (vibrational entropy) (S_{vib})**

- **Number of different bonding topologies (configurational entropy) (S_{conf})**

$$S_{xt} - S_{fluid}$$

SAPIENZA
UNIVERSITÀ DI ROMA

COLLDENSE
COLLOIDS with
DESIGNED RESPONSE

S_{xt} --- Crystal Vibrational Entropy S_{vib}

S_{fluid} --- Fluid Vibrational Entropy S_{vib} +

Fluid Configurational Entropy S_{conf}

$$S_{xt} - S_{fluid}$$

Increasing the bond angle increases both entropies…..
Same rate ?

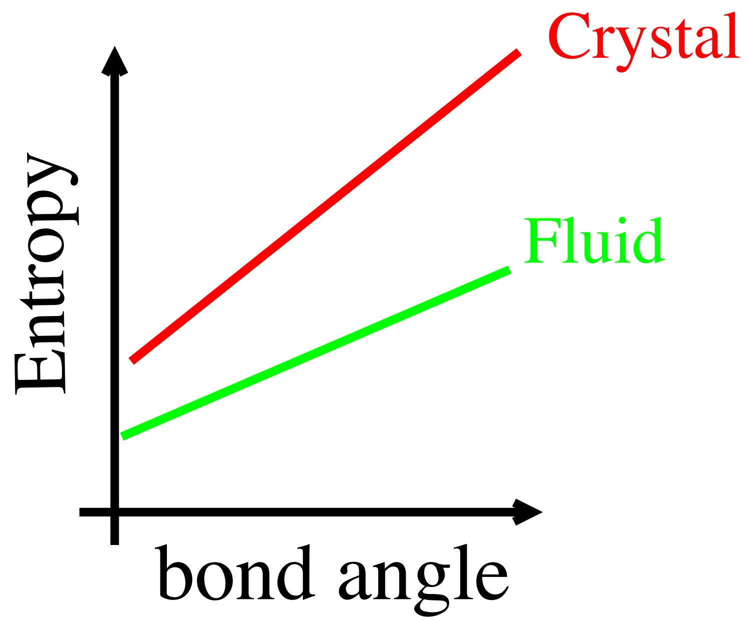

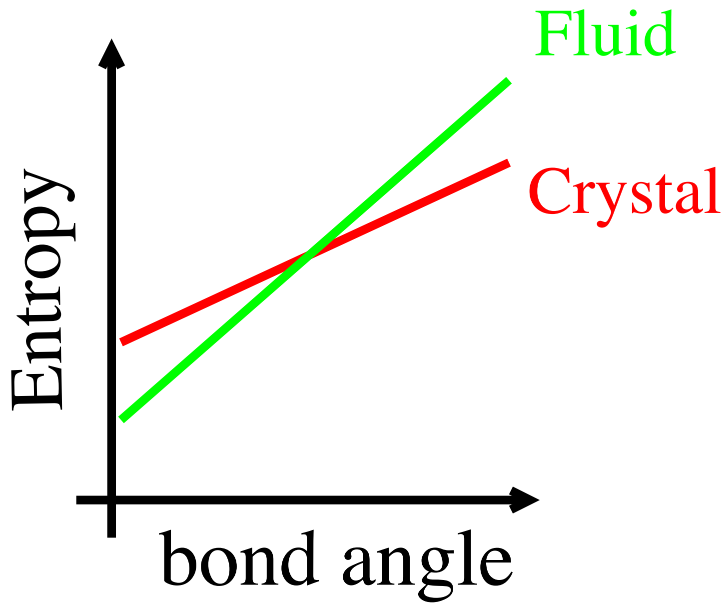

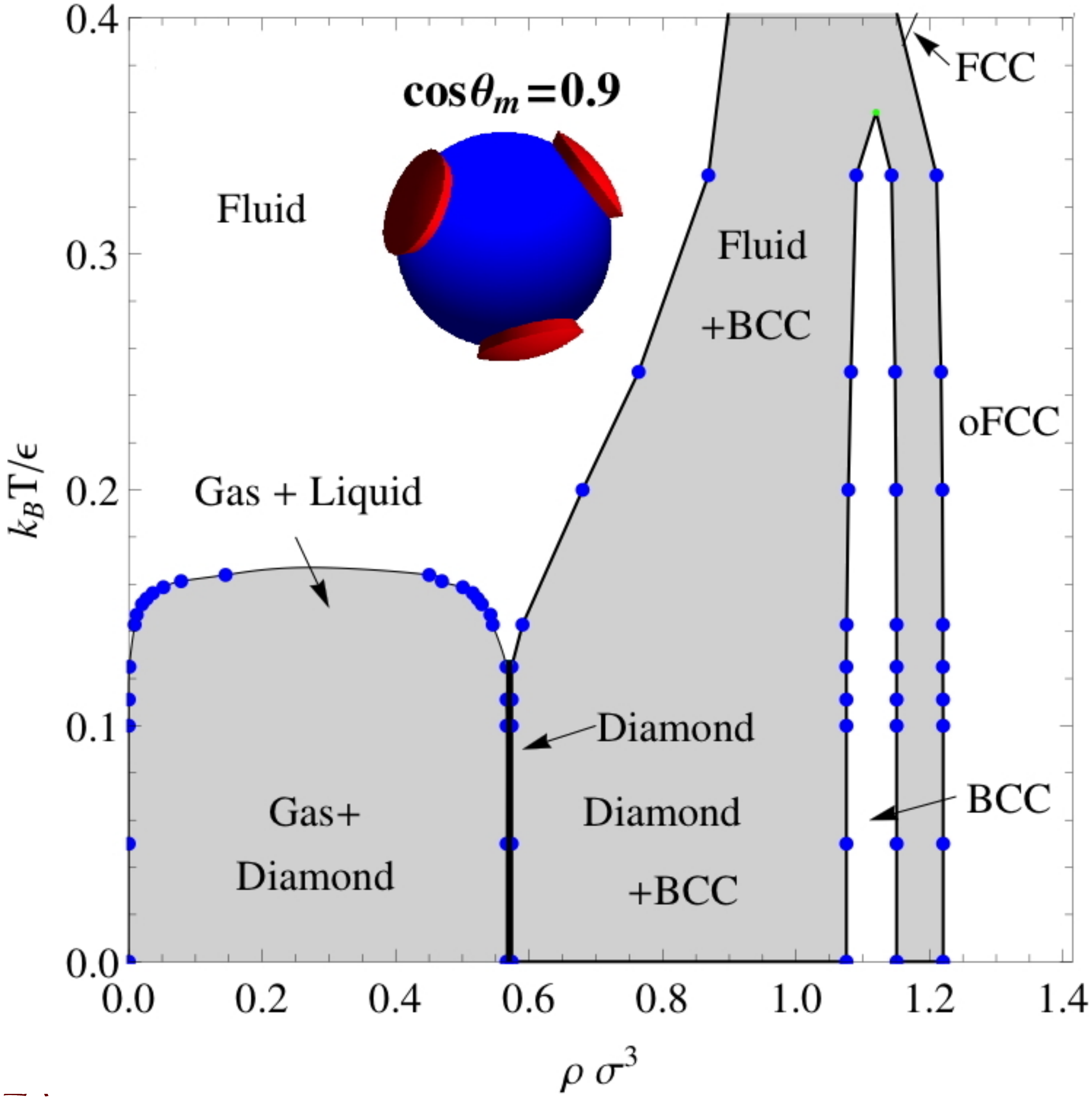
cosθm=0.9
Fluid
Gas + Liquid
Fluid
+BCC
FCC
oFCC
Diamond
Diamond
+BCC
BCC
Gas+
Diamond
0.4
0.3
0.2
0.1
0.0
0.0
0.2
0.4
0.6
0.8
1.0
1.2
1.4
kBT/ϵ
ρ σ3

On increasing flexibility: Ultrastable liquids !

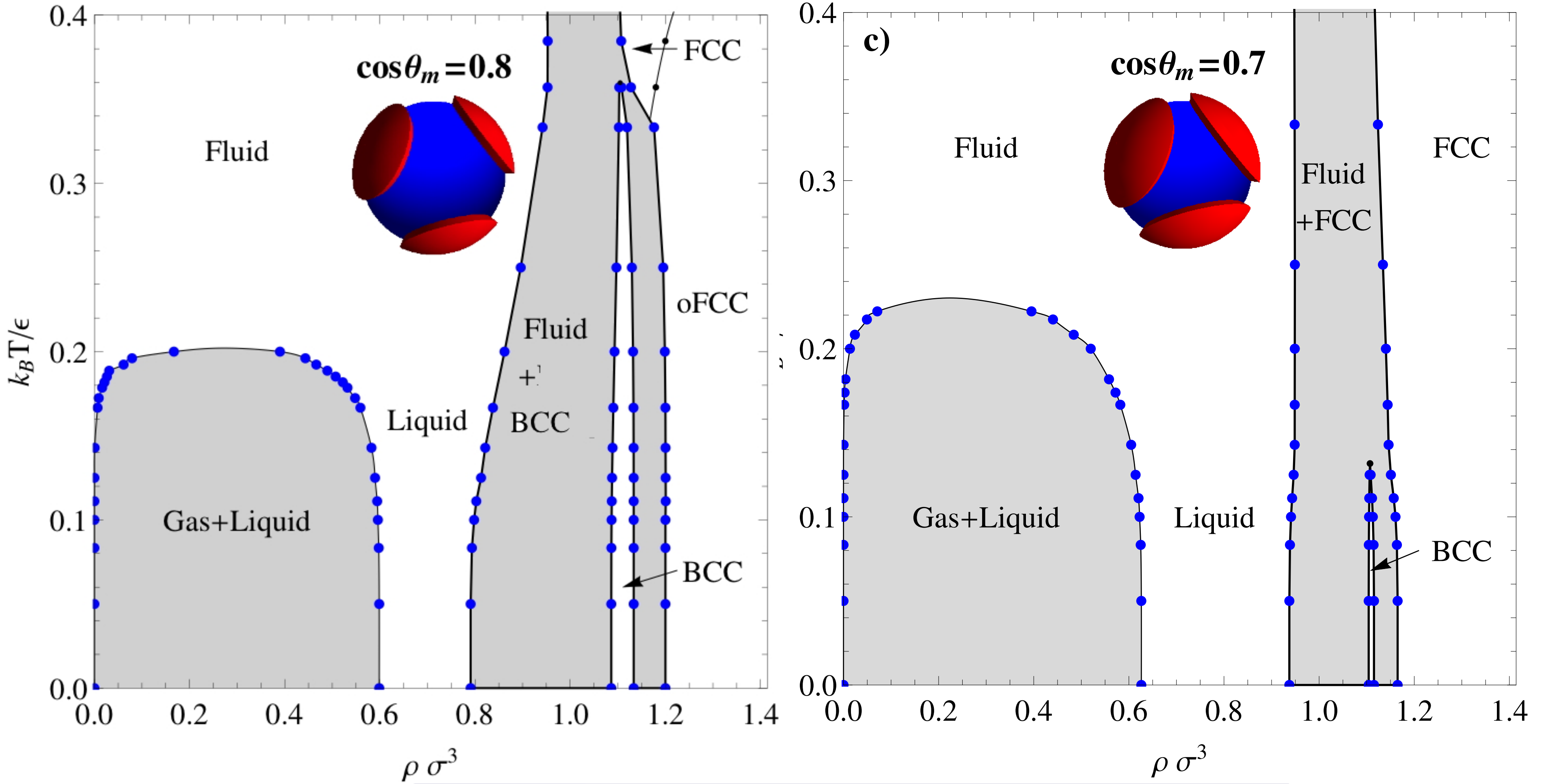

nature physics

LETTERS

Liquids more stable than crystals in particles with limited valence and flexible bonds

Frank Smallenburg* and Francesco Sciortino

SAPIENZA
UNIVERSITÀ DI ROMA

COLLDENSE
COLLOIDS with
DESIGNED RESPONSE

Key elements for liquid stability at T=0 K: (ultrastable liquids !)

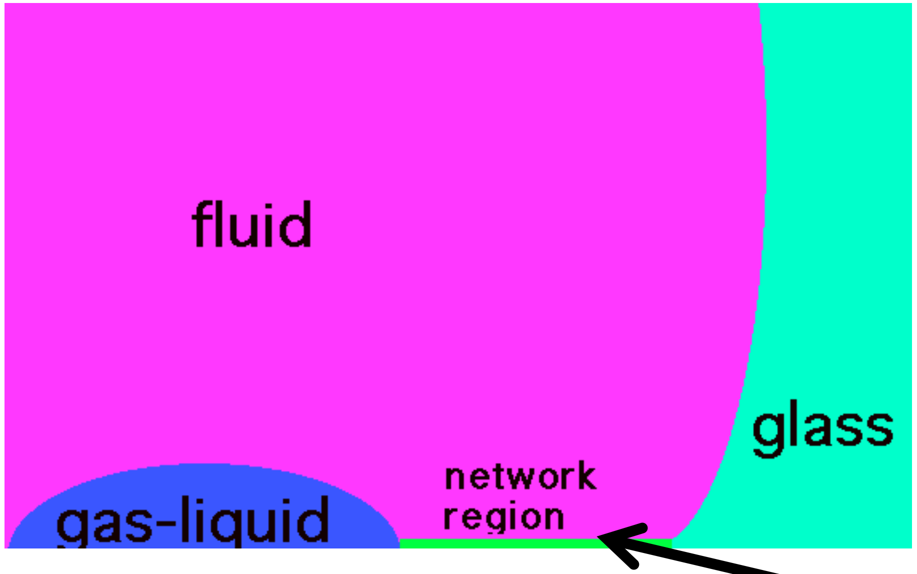

Thermodynamically stable !

- **Large flexibility of the angular interactions: (wide variety of networks, increasing S_{conf})**

- **Low valence. Small density of the coexisting liquid phase**

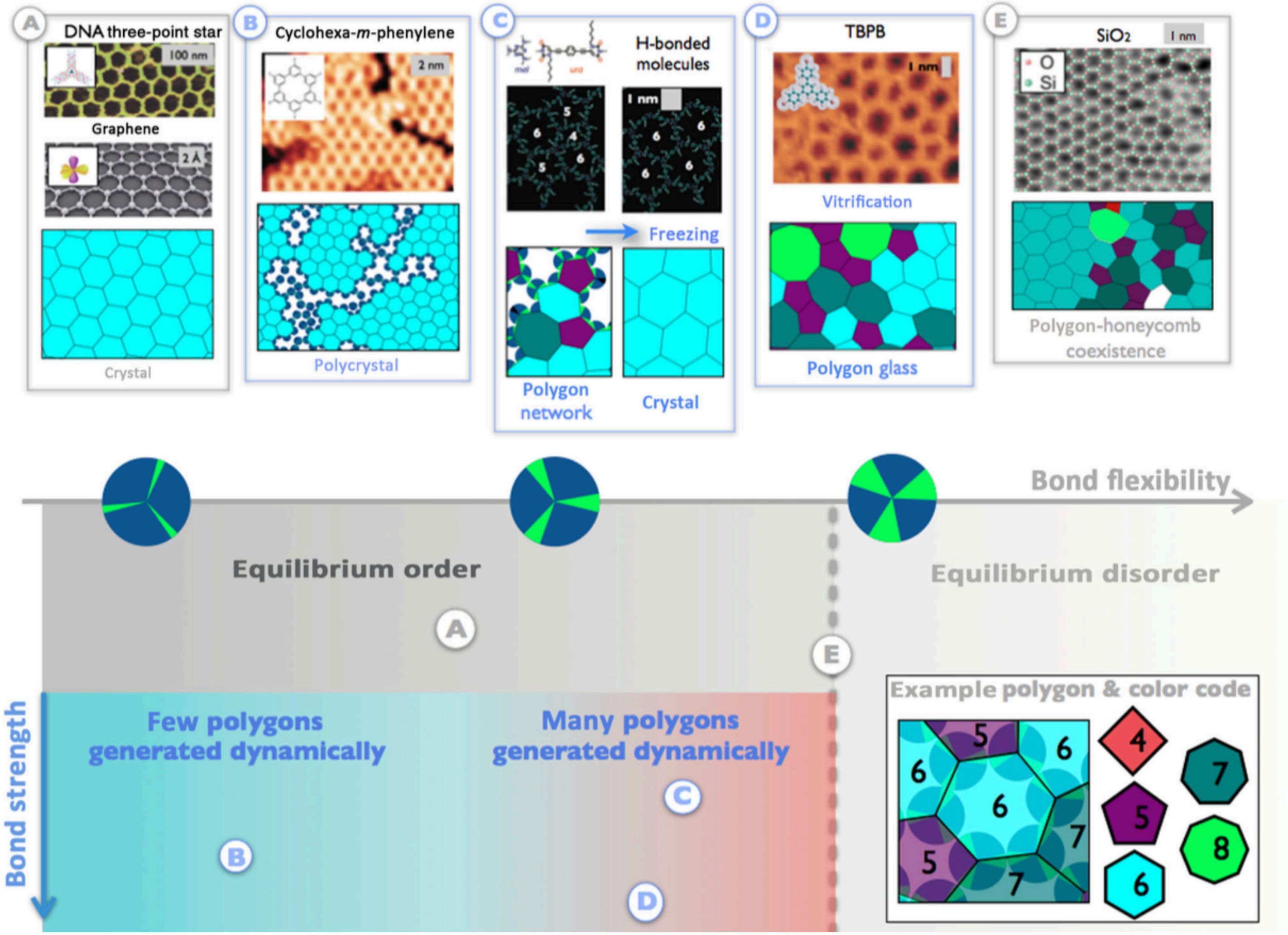

PHYSICAL REVIEW X **4,** 011044 (2014)

Common Physical Framework Explains Phase Behavior and Dynamics of Atomic, Molecular, and Polymeric Network Formers

Stephen Whitelam,[1,*] Isaac Tamblyn,[2,†] Thomas K. Haxton,[1] Maria B. Wieland,[3] Neil R. Champness,[4]
Juan P. Garrahan,[3] and Peter H. Beton[3,‡]

Crystal Selection by Entropy

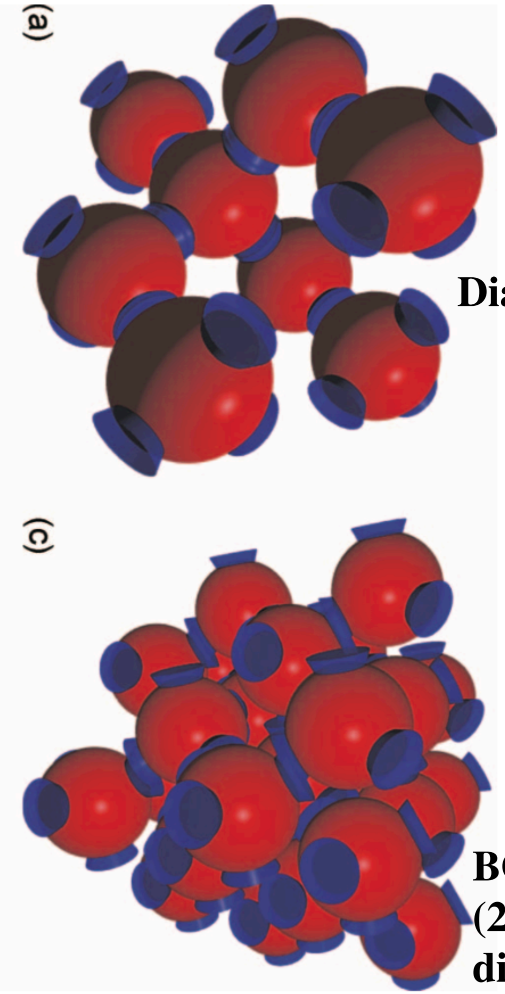

Diamond

BCC (2 interpenetrated diamond)

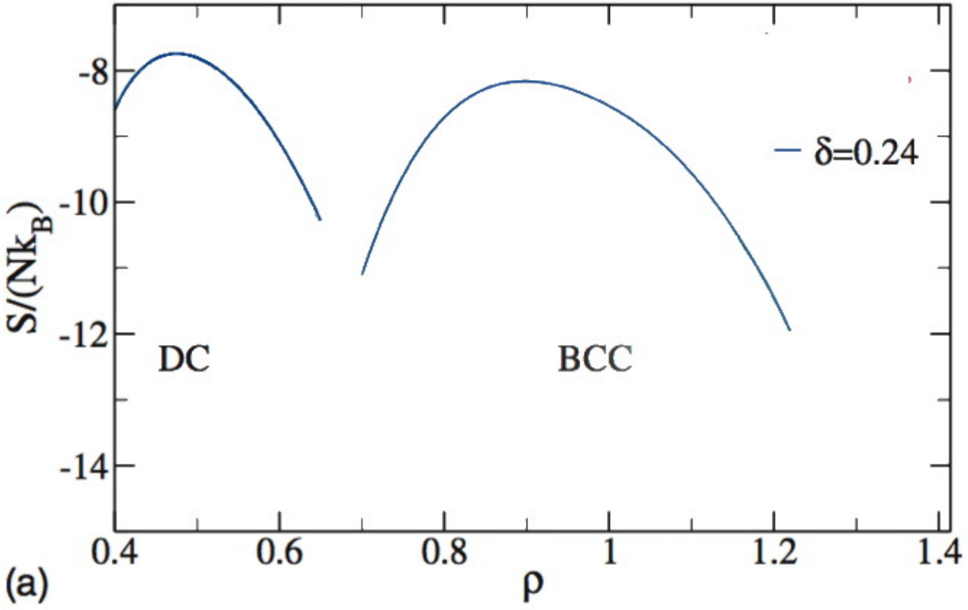

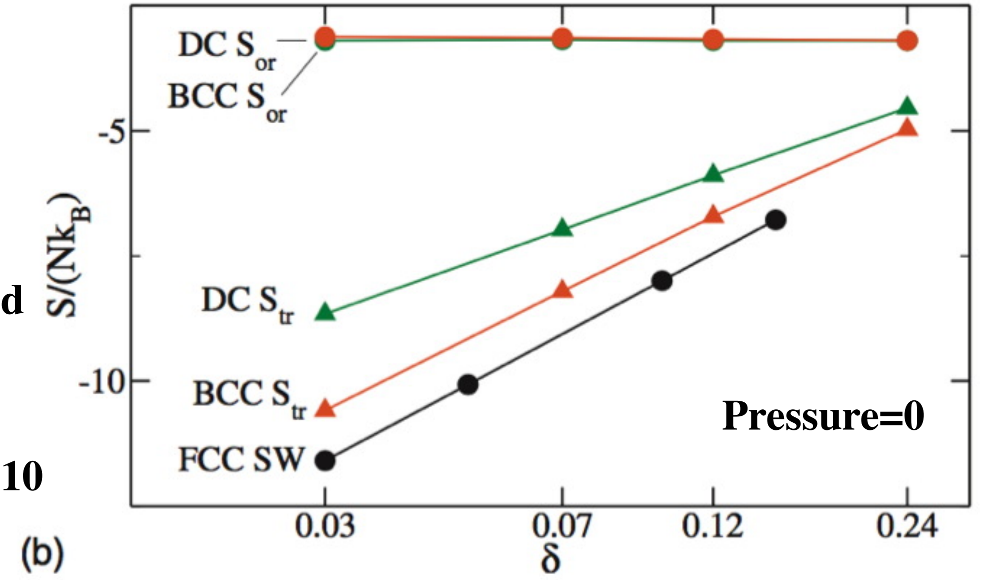

J. Chem. Phys 132, 184501 **2010**

Crystal Selection by Entropy

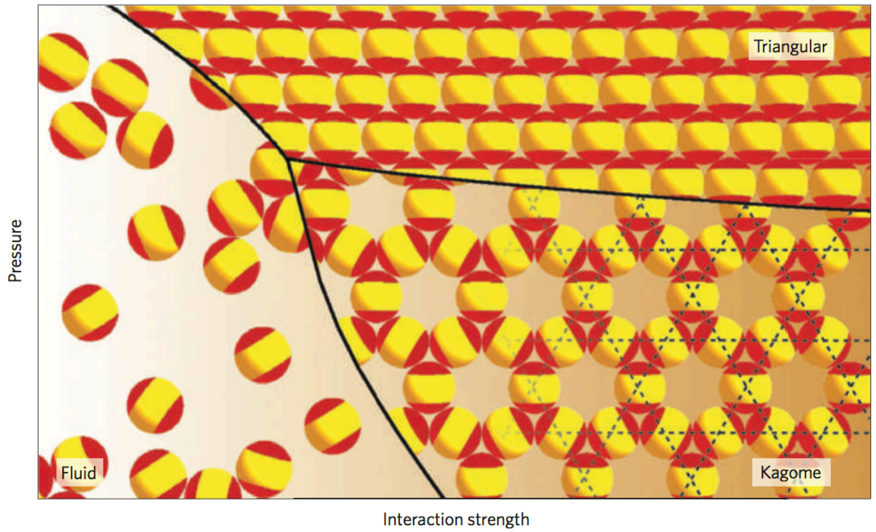

Figure 1 | Sketch of the phase diagram of triblock Janus particles[6]. Self-assembly occurs when the strength of the interaction between patches (depicted in red) is large enough to overcome the random forces arising from the thermal jiggling of the particles. In this case they crystallize into a kagome lattice, or a closed-packed triangular lattice at higher density.

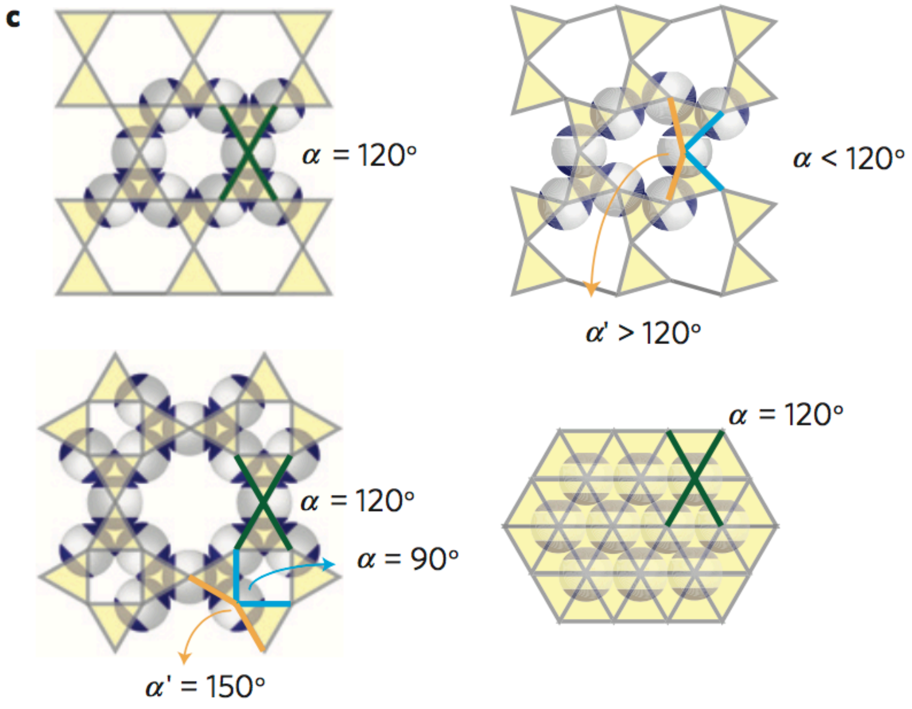

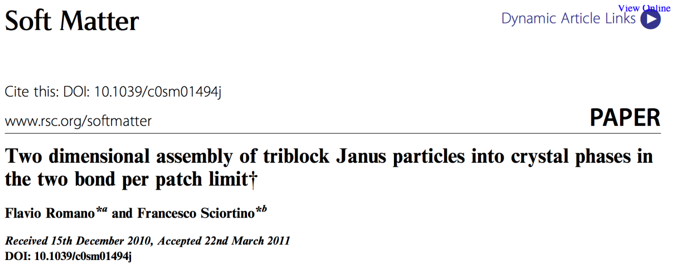
Soft Matter
Dynamic Article Links View Online

Cite this: DOI: 10.1039/c0sm01494j
www.rsc.org/softmatter
PAPER

Two dimensional assembly of triblock Janus particles into crystal phases in the two bond per patch limit†

Flavio Romano[*a] and Francesco Sciortino[*b]

Received 15th December 2010, Accepted 22nd March 2011
DOI: 10.1039/c0sm01494j


nature materials
LETTERS
PUBLISHED ONLINE: 13 JANUARY 2013 | DOI: 10.1038/NMAT3496

Entropy favours open colloidal lattices

Xiaoming Mao[1,2]★, Qian Chen[3] and Steve Granick[3,4,5]

Crystal Selection by Entropy

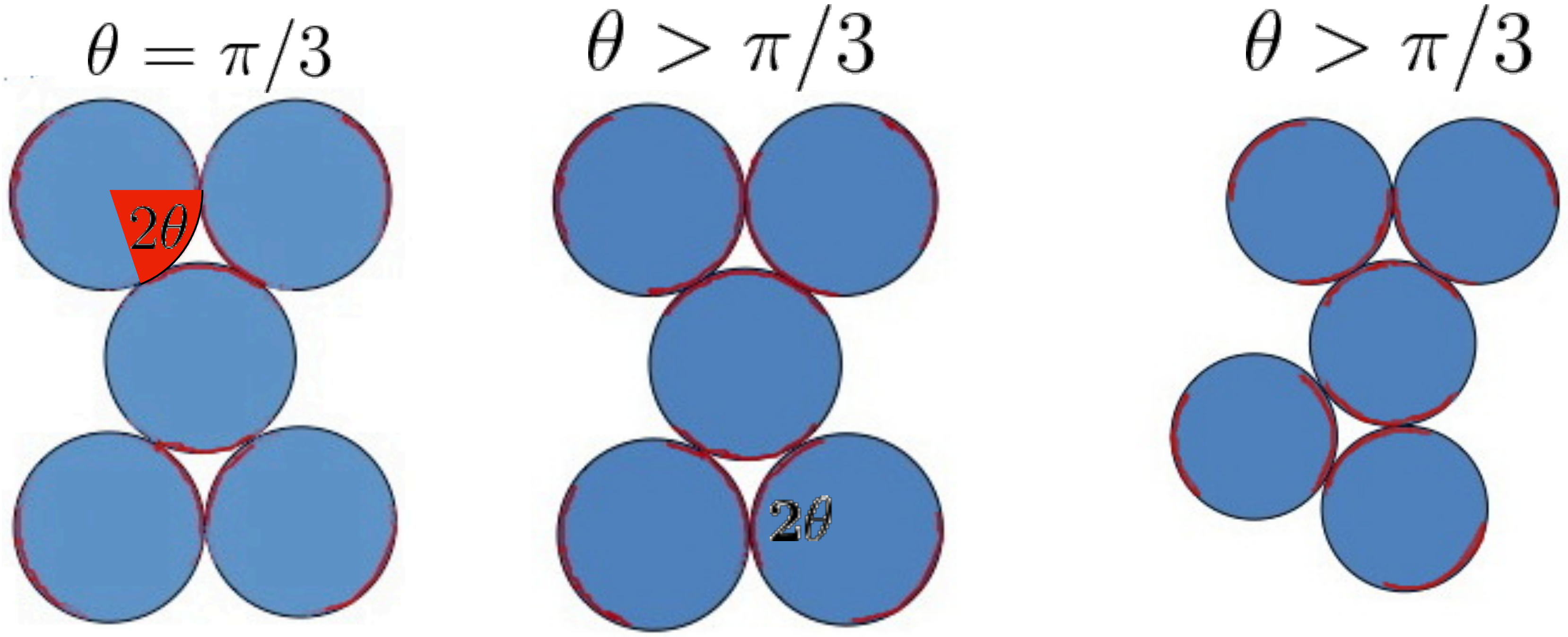

$\Theta = 0$ $\Theta = 2\theta - \pi/3$ $\Theta < 2\theta - \pi/3$

2θ = patch width

Θ = free rotation angle


nature materials
LETTERS
PUBLISHED ONLINE: 13 JANUARY 2013 | DOI: 10.1038/NMAT3496

Entropy favours open colloidal lattices

Xiaoming Mao[1,2]*, Qian Chen[3] and Steve Granick[3,4,5]

Entropic disparity

$\zeta = L_1 / L_2$

Optimizing the formation of solid solutions with components of different shapes

Fernando A. Escobedo

Citation: The Journal of Chemical Physics **146**, 134508 (2017); doi: 10.1063/1.4979091

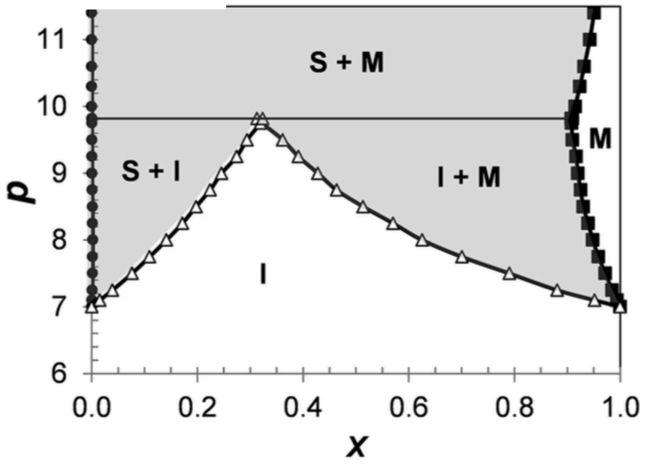

FIG. 4. Pressure-composition phase diagram for the hard-core mixture of octahedra + spheres for size ratio $\zeta = \sigma / a_8 = 0.836$ (equal ODP ~ 7). Phase

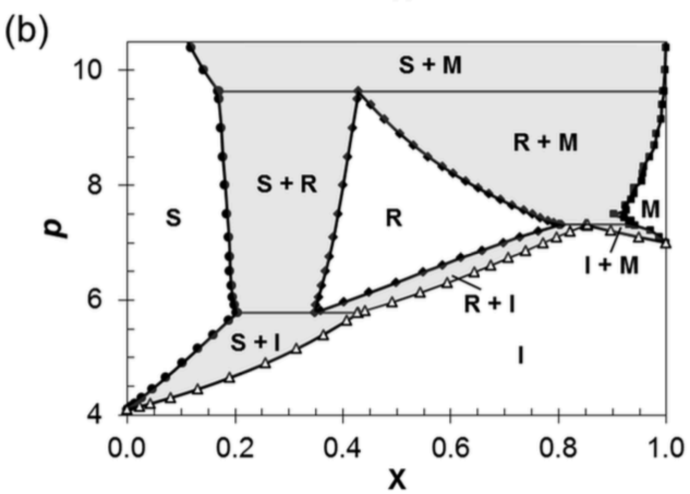

FIG. 5. Pressure-composition phase diagrams for hard-core mixtures of octahedra + spheres for (a) $\zeta = 0.955$ and (b) $\zeta = 1.0$. Areas shaded in

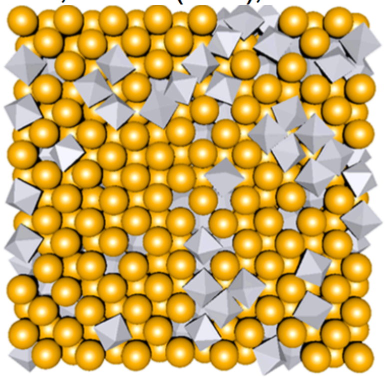

Spheres (S)

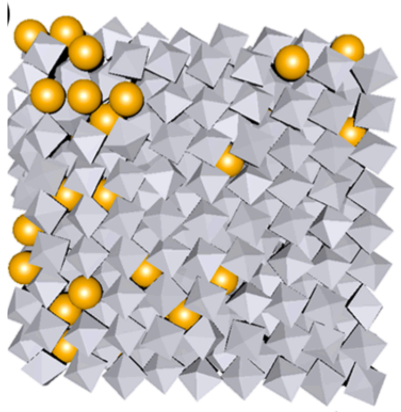

Octahedra (M)

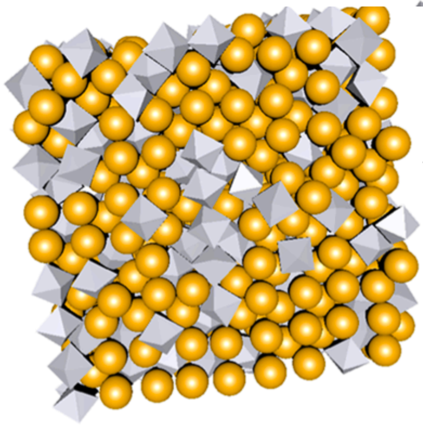

Mixed Spheres+ Octahedra (R)

COLLDENSE
COLLOIDS with DESIGNED RESPONSE

Predictive Self-Assembly of Polyhedra into Complex Structures

Pablo F. Damasceno,[1]* Michael Engel,[2]* Sharon C. Glotzer[1,2,3]†

SCIENCE VOL 337 27 JULY 2012

Dense Regular Packings of Irregular Nonconvex Particles

Joost de Graaf, René van Roij, and Marjolein Dijkstra

Phys. Rev. Lett. **107**, 155501 – Published 3 October 2011

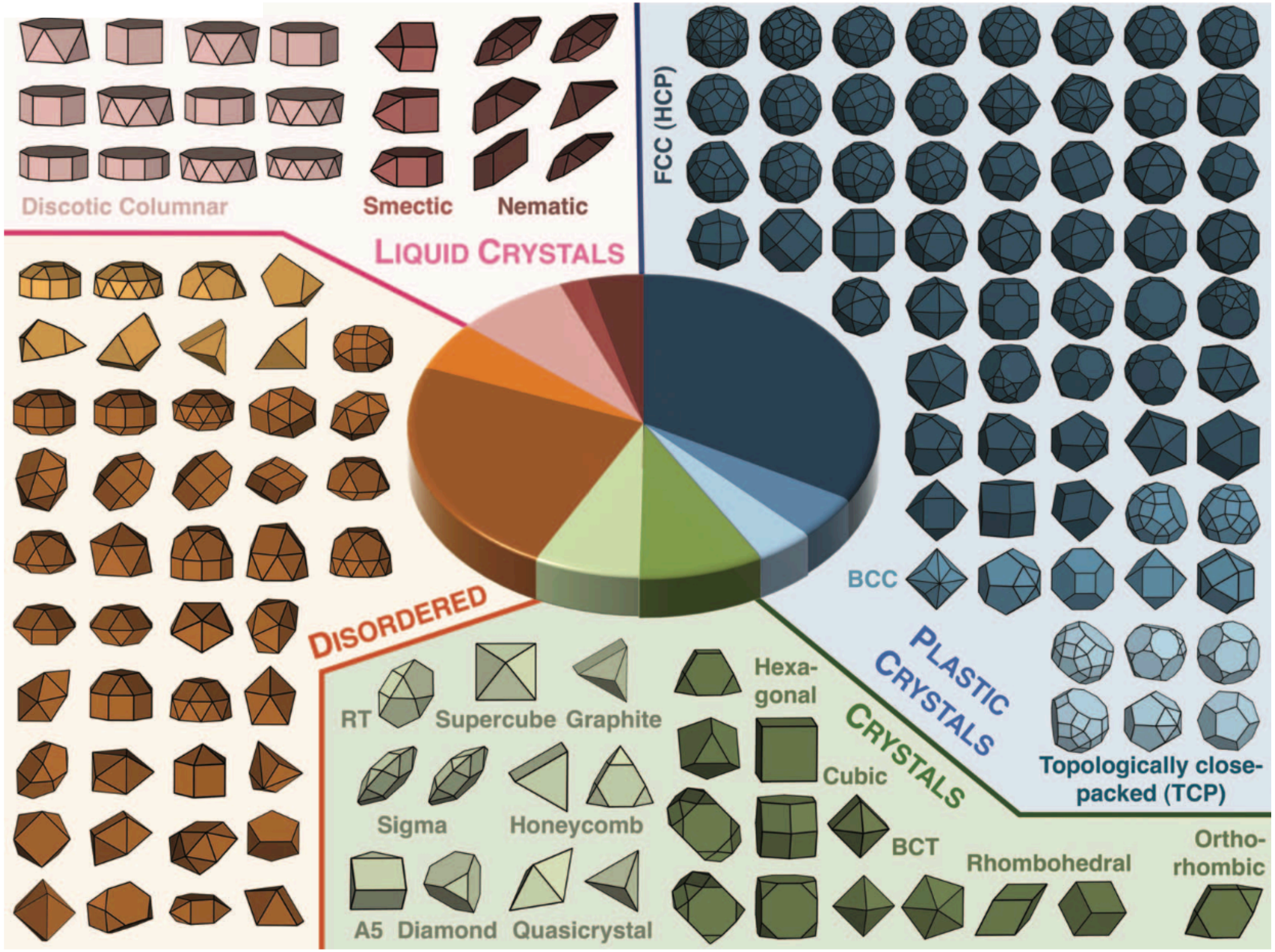

Fig. 1. Polyhedra are separated into four categories of organization as indicated by different colors:

Entropic Attraction
Large HS in a bath of small HS

Which distance is most probable ?

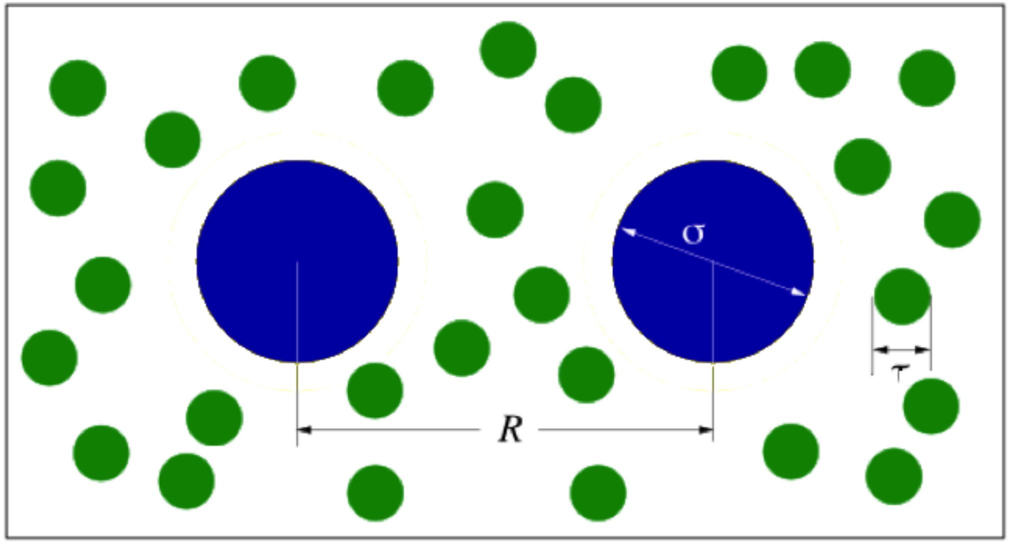

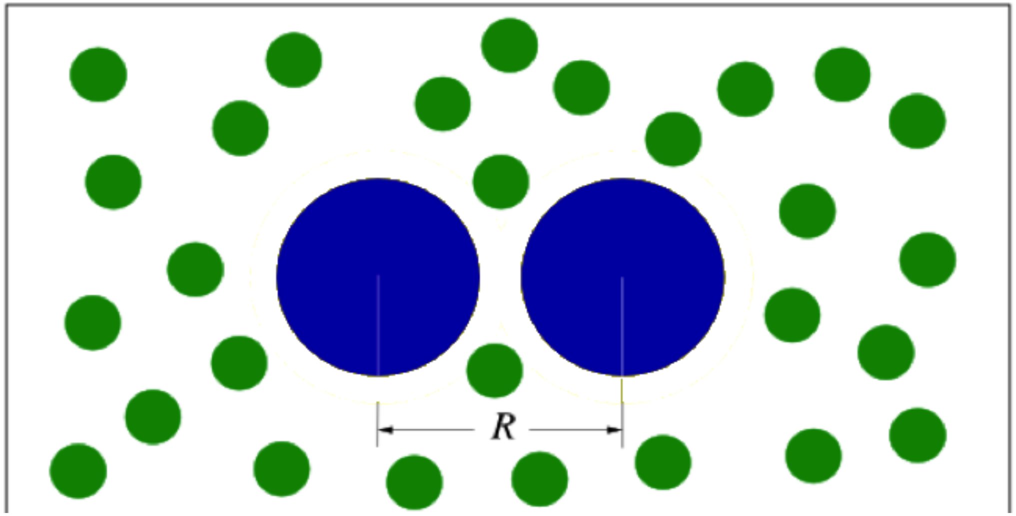

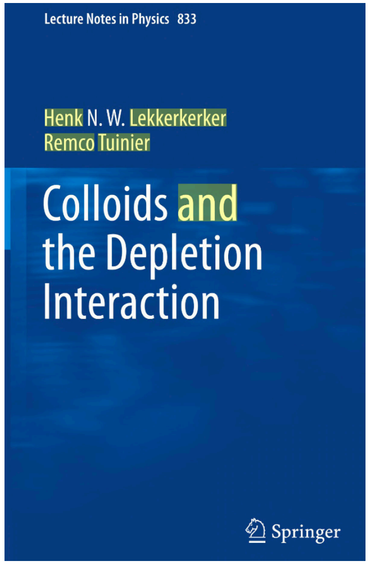

Lecture Notes in Physics 833

Henk N. W. Lekkerkerker
Remco Tuinier

Colloids and the Depletion Interaction

Springer

Depletion interaction

$$\boxed{S \sim n_{\text{poly}} \ln V}$$

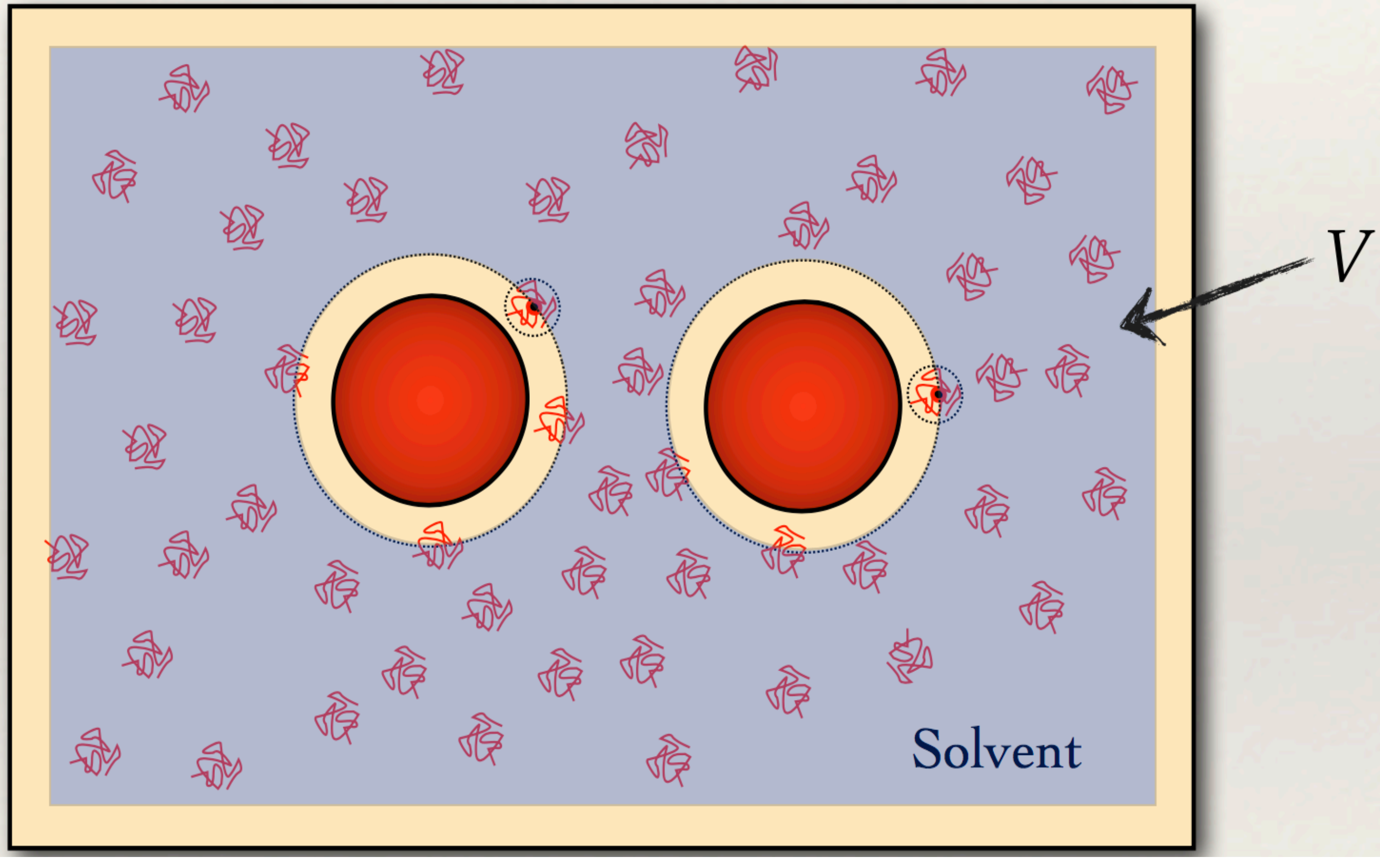

$$S \sim n_{\mathrm{poly}} \ln V$$

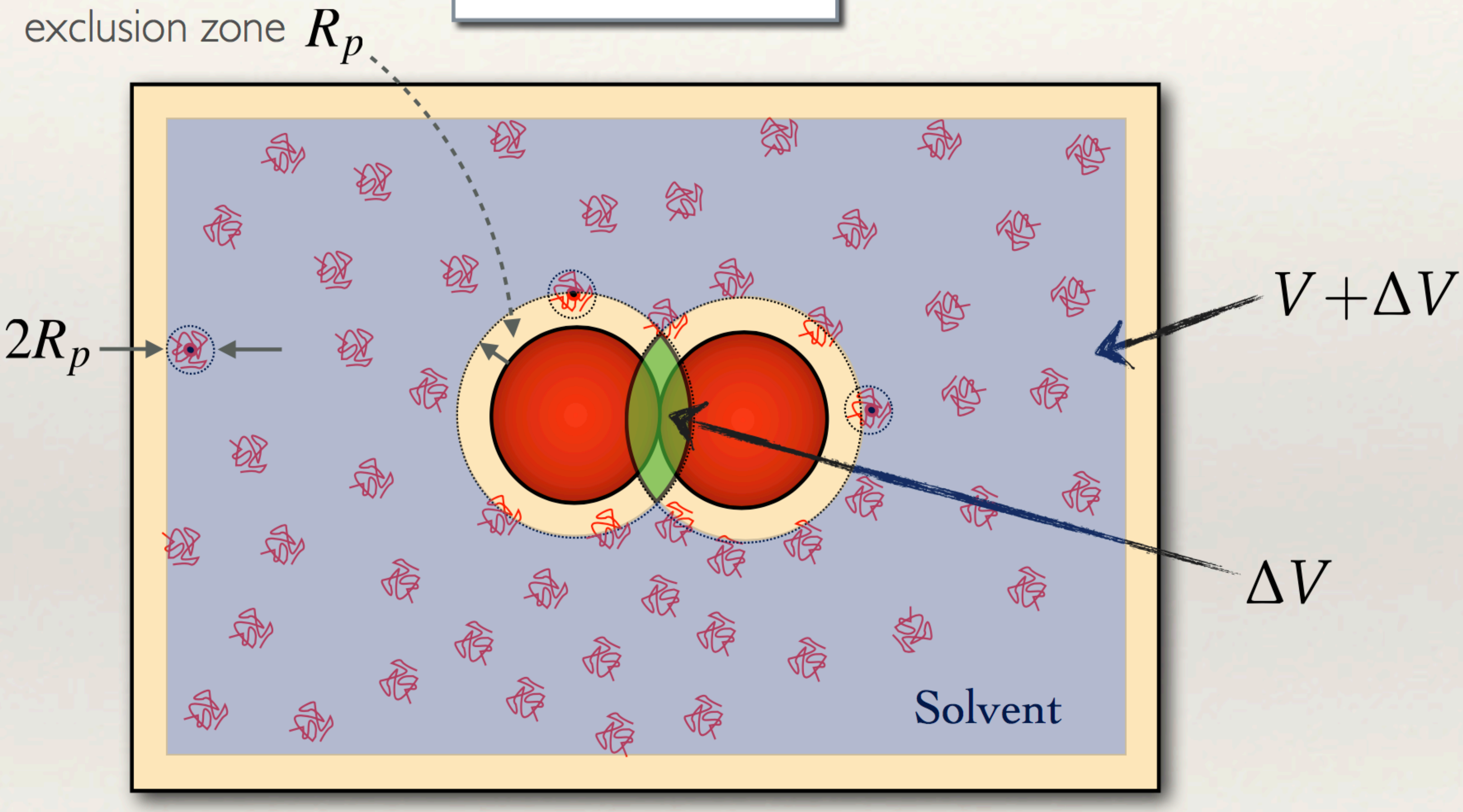

$$\Delta S \sim n_{\mathrm{poly}} \frac{\Delta V}{V}$$

sawa, J. Chem. Phys. **22**, 1255 (1954).

Let's assume we have N large HS and M small HS. The partition function in the NVT ensamble is

$$Q_{N+M} = \frac{1}{N!\lambda_N^{3N}} \frac{1}{M!\lambda_M^{3M}} \int d\vec{r}_1 ... d\vec{r}_N \int d\vec{s}_1 ... d\vec{s}_M e^{-\beta(V_{11}(\vec{r}^N)+V_{12}(\vec{r}^N,\vec{s}^M)+V_{22}(\vec{s}^M))}$$

and let's define

$$e^{-\beta V_{eff}(\vec{r}^N)} \equiv \frac{1}{M!\lambda_M^{3M}} \int d\vec{s}_1 ... d\vec{s}_M e^{-\beta(V_{12}(\vec{r}^N,\vec{s}^M)+V_{22}(\vec{s}^M))}$$

such that

$$Q_{N+M} = \frac{1}{N!\lambda_N^{3N}} \int d\vec{r}_1 ... d\vec{r}_N e^{-\beta V_{11}(\vec{r}^N)} e^{-\beta V_{eff}(\vec{r}^N)}$$

The total interaction potential felt by the large HS is thus the sum of the direct interaction plus (a T and ρ dependent) effective potential.

$$V_{tot}(\vec{r}^N) = V_{11}(\vec{r}^N) + V_{eff}(\vec{r}^N)$$

1 Asakura-Oosawa for two colloids

If $N = 2$ and if we assume $V_{22} = 0$, but retaining the excluded volume interaction for V_{12}

Small-large

Small-small

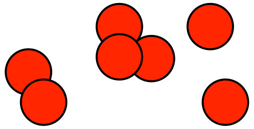

$$e^{-\beta V_{eff}(\vec{r}_1,\vec{r}_2)} = \frac{1}{M!\lambda_M^{3M}} \int d\vec{s}_1 ... d\vec{s}_M e^{-\beta V_{12}(\vec{r}_1,\vec{r}_2,\vec{s}^M)}$$

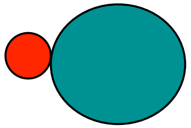

Since

$$V_{12}(\vec{r}_1, \vec{r}_2, \vec{s}^M) = \sum_{j=1}^{M} v_{12}(\vec{r}_1, \vec{r}_2, \vec{s}_j)$$

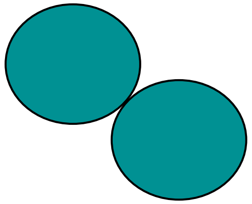

then

$$e^{-\beta V_{eff}(\vec{r}_1,\vec{r}_2)} = \frac{1}{M!\lambda_M^{3M}} \left[\int d\vec{s}_1 e^{-\beta v_{12}(\vec{r}_1,\vec{r}_2,\vec{s}_1)} \right]^M$$

SAPIENZA
UNIVERSITÀ DI ROMA

Asakura, S., Oosawa,F, On Interaction between Two Bodies Immersed in a Solution of Macromolecules, JCP 22 (7): 1255 1954.

COLLDENSE
COLLOIDS with DESIGNED RESPONSE

$$V_0 \equiv \frac{4\pi}{3}\left(\frac{\sigma_c+\sigma_p}{2}\right)^3$$

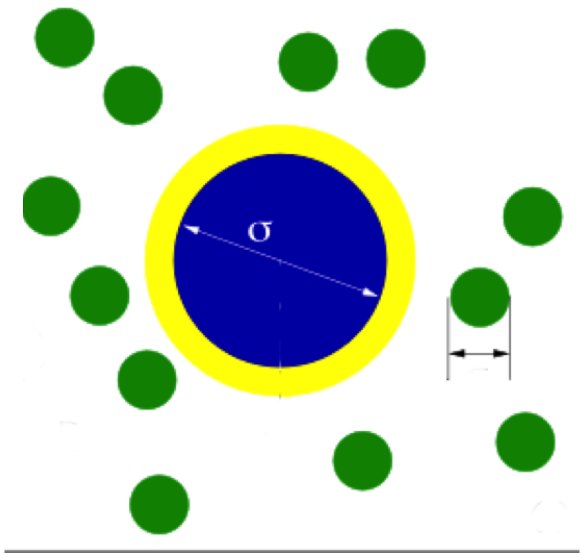

$$\int d\vec{s}_1 e^{-\beta v_{12}(\vec{r}_1,\vec{r}_2,\vec{s}_1)} = V - 2V_0 + V_{overlap}(|\vec{r}_1-\vec{r}_2|)$$

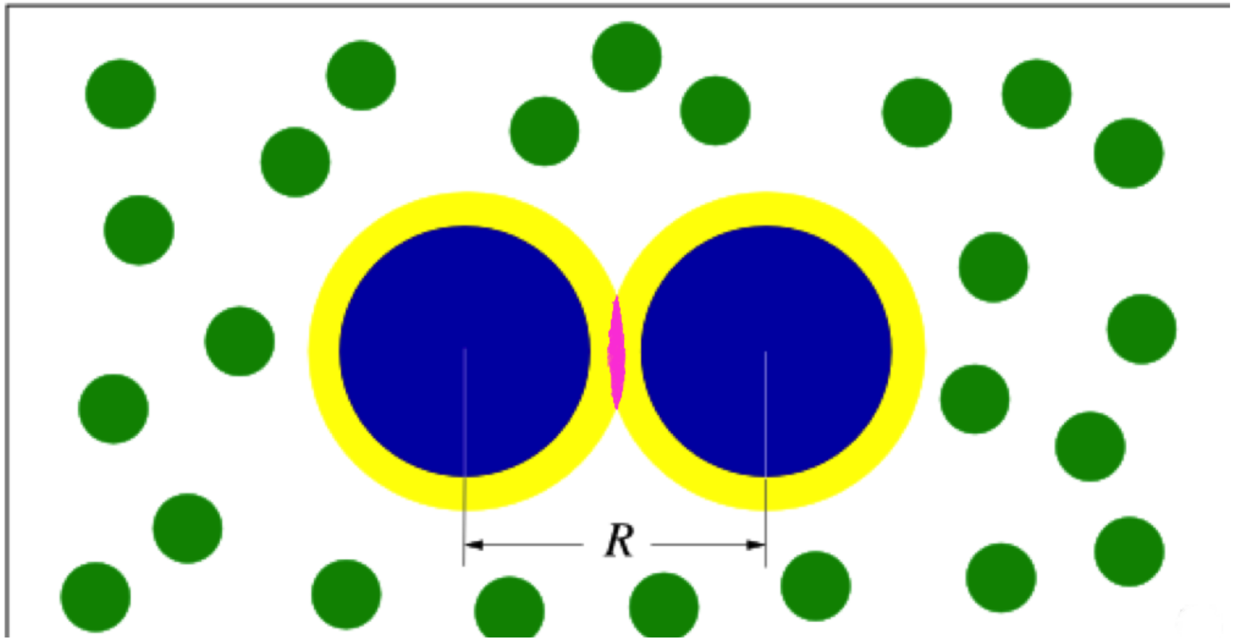

$$e^{-\beta V_{eff}(R)} = \frac{1}{M!\lambda_M^{3M}}\left[V - 2V_0 + V_{overlap}(R)\right]^M = \frac{(V-2V_0)^M}{M!\lambda_M^{3M}}\left[1+\frac{V_{overlap}(R)}{V-2V_0}\right]^M \approx$$

$$\frac{(V-2V_0)^M}{M!\lambda_M^{3M}}\left(1+\frac{M}{V-2V_0}V_{overlap}(R)\right)$$

where $M/(V-2V_0) \equiv \rho_M$ is the number density of small spheres. Hence

$$-\beta V_{eff}(R) = -M\left[\ln(\rho_M\lambda_M^3) - 1\right] + \ln(1+\rho_M V_{overlap}(R)).$$

Expanding the logarithm ($\ln(1+x) \approx -x$)

$$\beta V_{eff}(R) = V\rho_M\left[\ln(\rho_M\lambda_M^3) - 1\right] - \rho_M V_{overlap}(R)$$

Thus, beside a R-independent term, there is an entropic effective interaction which can be written (recognising $k_B T\rho_M$ as the ideal gas pressure Π exerted by the small particles)

$$V_{eff}(R) = -k_B T\rho_M V_{overlap}(R) = -\Pi V_{overlap}(R)$$

Sphere-Sphere Intersection

DOWNLOAD
Mathematica Notebook

$$u(r) = \begin{cases} \infty & 0 < r < \sigma \\ -\Pi V_{overlap} & \sigma < r < \sigma + \tau \\ 0 & r > \sigma + \tau \end{cases}$$

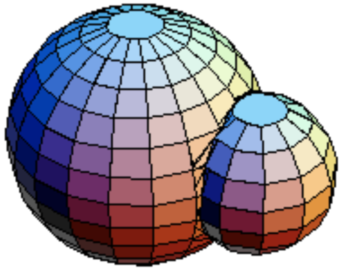

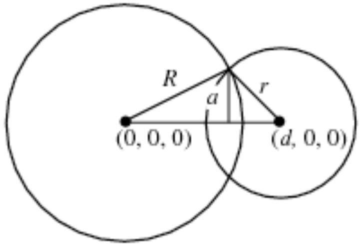

Letting $R_1 = R$ and $R_2 = r$ and summing the two caps gives

$$V = V(R_1, h_1) + V(R_2, h_2) = \frac{\pi (R + r - d)^2 (d^2 + 2 d r - 3 r^2 + 2 d R + 6 r R - 3 R^2)}{12 d}.$$

$$V_{overlap} = \frac{\pi}{12}[2(\sigma + \tau) + r)][(\sigma + \tau) - r]^2$$

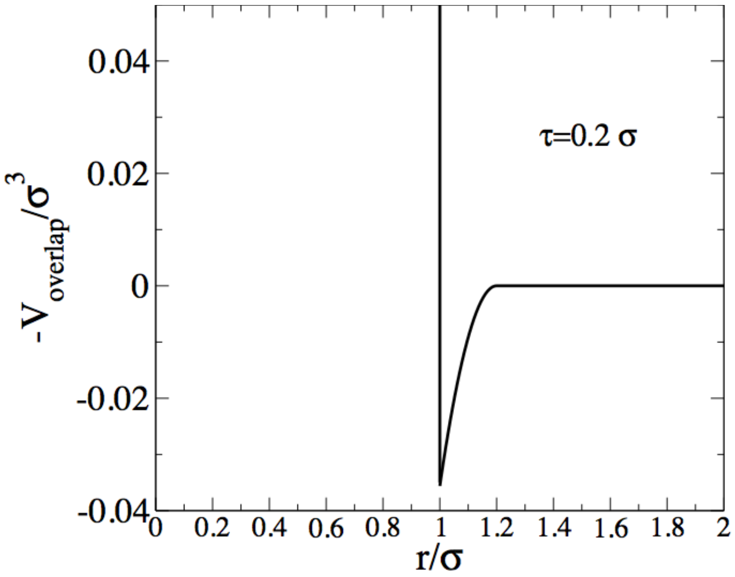

Same story from a different perspective

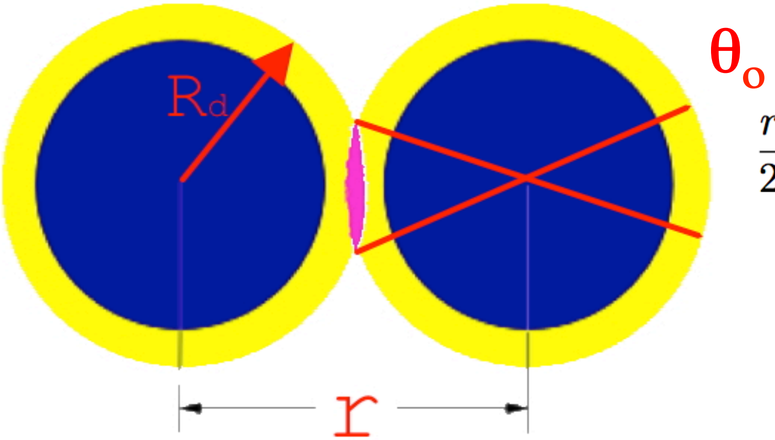

$$\frac{r}{2} = R_d \cos\theta_0 \quad \rightarrow \quad \cos\theta_0 = \frac{r}{2R_d}$$

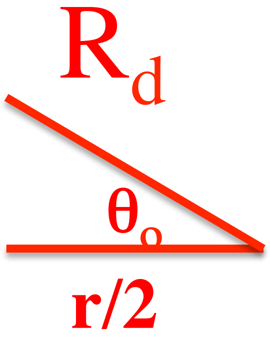

$$d\vec{F} = -P d\vec{a} \qquad da = R_d^2 sin\theta d\theta d\phi$$

$$dF_x = -|d\vec{F}|\ cos\theta$$

$$F_x(r) = \int_{-\theta_0}^{\theta_0} dF_x = -PR_d^2 \int_0^{2\pi} \int_{-\theta_0}^{\theta_0} cos\theta sin\theta d\theta d\phi = -2\pi PR_d^2[1 - cos(\theta_0)^2] = -2\pi PR_d^2 \left[1 - \left(\frac{r}{2R_d}\right)^2\right]$$

$$V(r) = -\int_{2R_d}^{r} F_x(r')dr'$$

Real hard-spheres

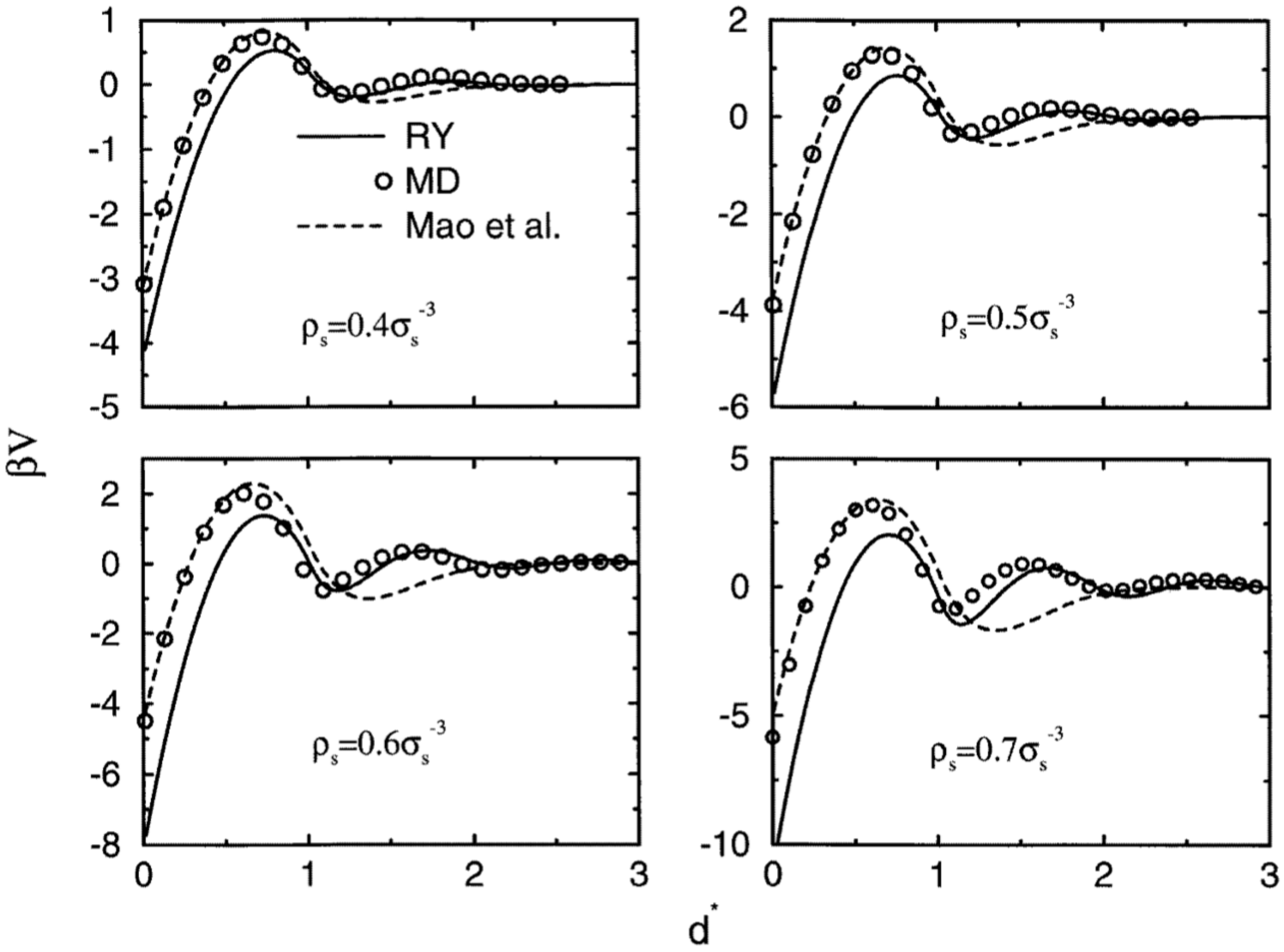

Figure 9. The effective depletion potential as a function of the density of small particles. This figure shows a comparison between MD data, the theory of Mao *et al* [2], and the superposition approximation using the RY pair distribution functions. In every case, the short-distance behaviour coincides with the perturbation theory of reference [2], and the long-range behaviour compares very well with the superposition approximation.

Visualizzation of depletion forces

Phase separation of a bidisperse sphere mixture:

$r_b = 413$nm, $r_s = 35$nm,

Volume fraction: $\Phi_b = 0.02$
(visible),
(not resolved)

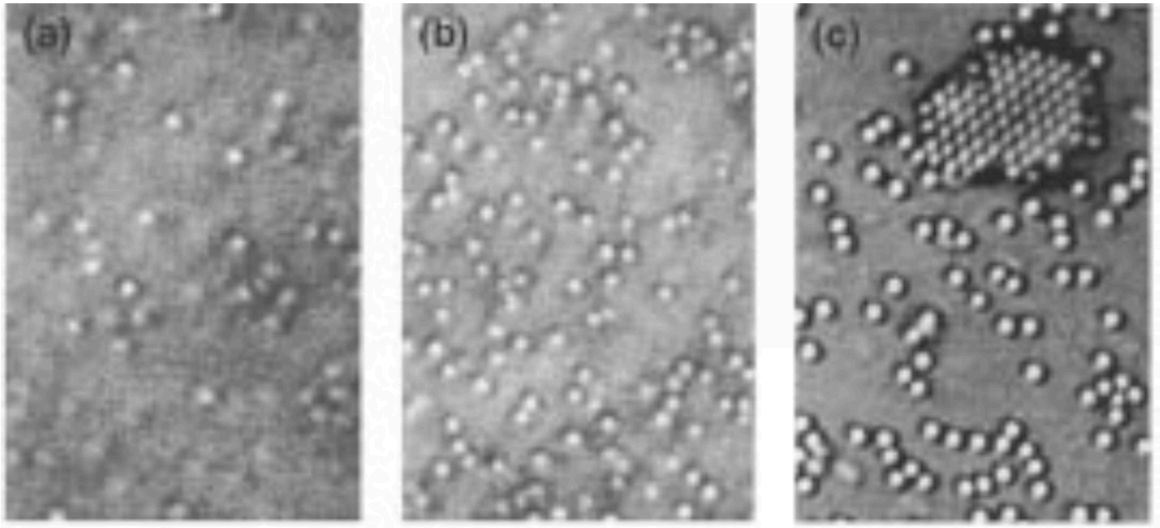

Fig. 1. – Optical micrographs of polystyrene spheres ($r_1 = 0.413$ µm, $\phi_1 = 0.02$) at a flat, glass wall. (a) With no small spheres, a low area fraction of spheres (η_1^{wall}) is seen. The spheres remain in view for much less than a second before diffusing away into the bulk. (b) When small spheres are added ($r_2 = 0.035$ µm, $\xi = .084$, $\phi_2 = 0.08$), η_1^{wall} increases. The large spheres diffuse along the surface for an average of minutes before escaping to the bulk. The small spheres are invisible. (c) With $\phi_2 = 0.16$, a crystallite made of the large spheres can be seen at the surface (after ≈ 40 h).

A.D. Dinsmore, P. B. Warren, W. C. K. Poon, and A. G. Yodh,
EPL 40, 337 (1997).

For depletion interactions, arrest at low ϕ (gelation) is the result of a phase separation process interrupted by the glass transition

Gelation of particles with short-range attraction

Peter J. Lu[1], Emanuela Zaccarelli[3,4], Fabio Ciulla[3], Andrew B. Schofield[5], Francesco Sciortino[3,4] & David A. Weitz[1,2]

Vol 453 | 22 May 2008 | doi:10.1038/nature06931

CONFOCAL IMAGES
First Order Transition

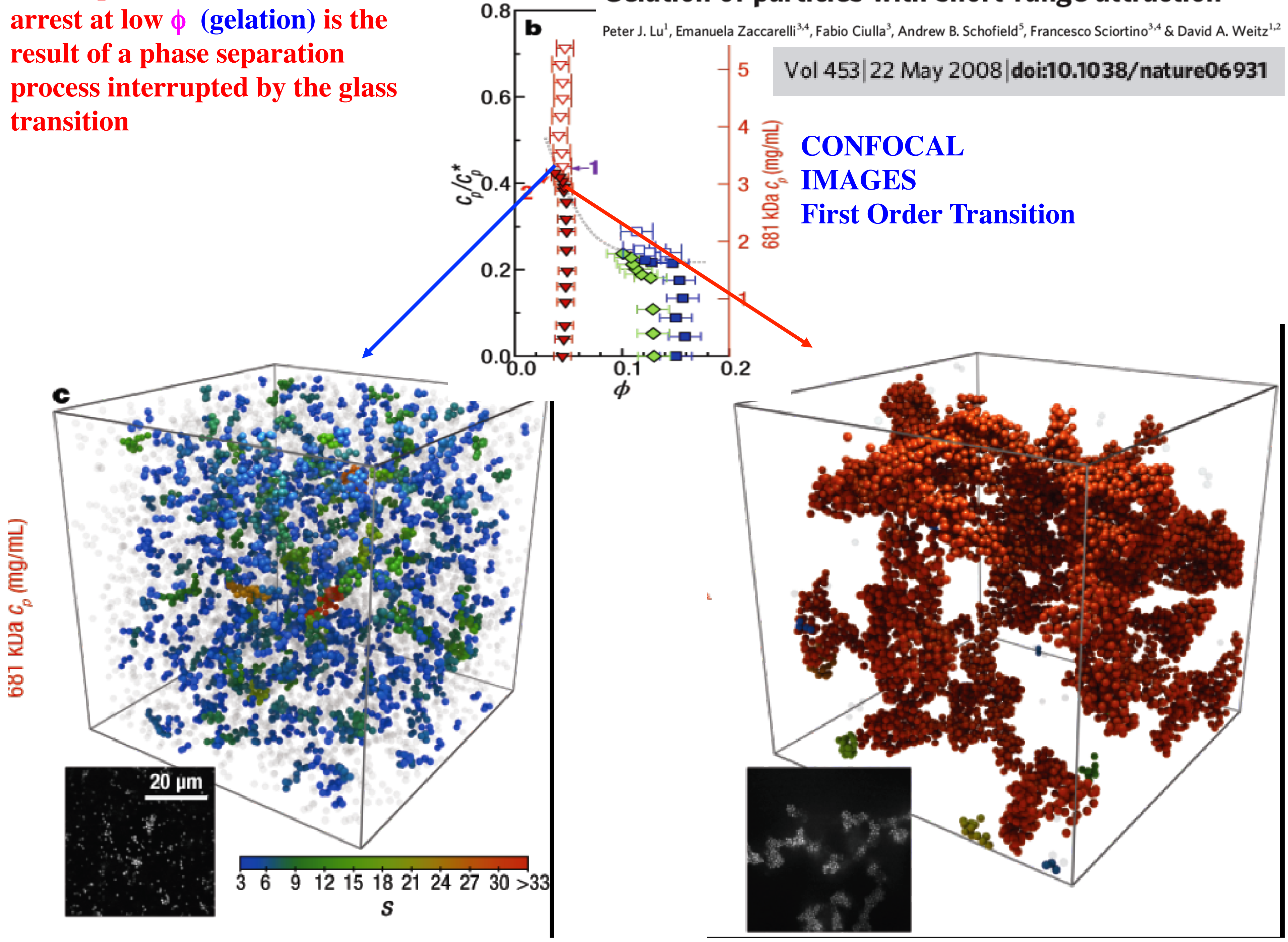

Depletion: shape and roughness

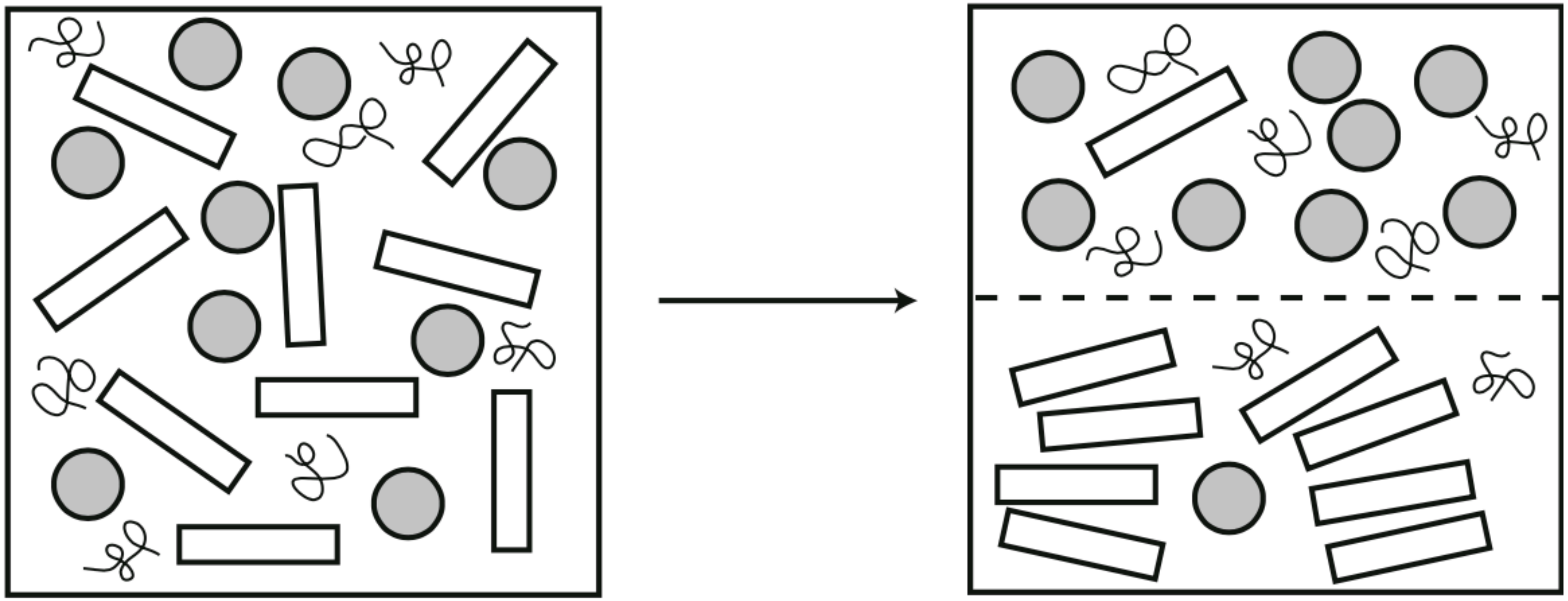

Fig. 1.28 Shape-selective separation induced by depletion forces

[redacted]

PHYSICAL REVIEW E **66**, 060402(R) (2002)

Osmotically driven shape-dependent colloidal separations

T. G. Mason
Corporate Strategic Research, ExxonMobil Research and Engineering Co., Route 22 East, Annandale, New Jersey 08801

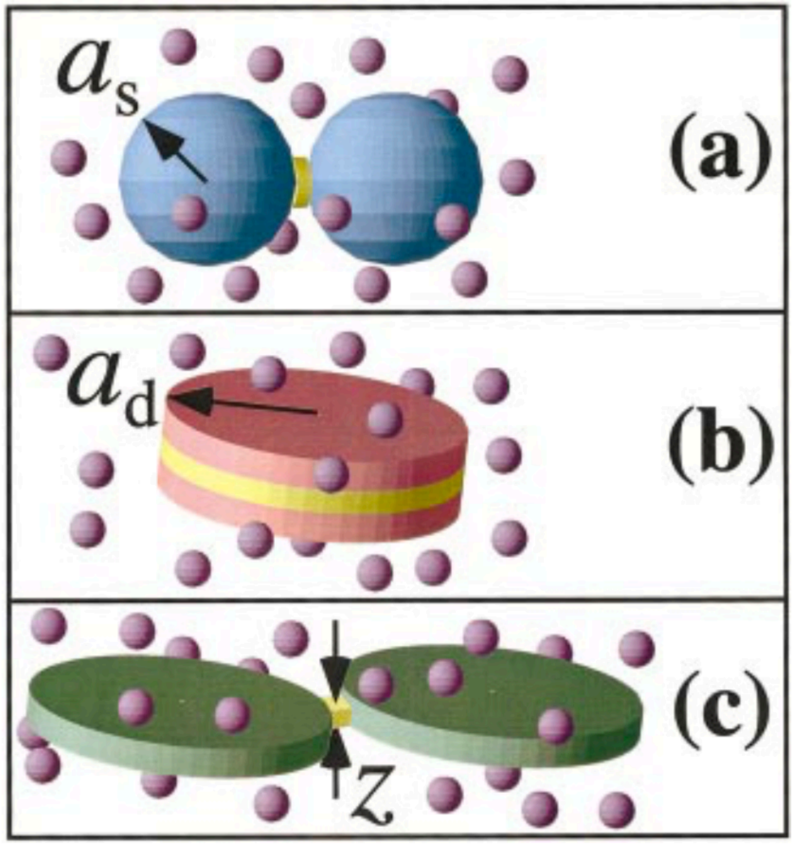

FIG. 3. (Color) Schematic representations of the excluded volumes (yellow) between (a) two spheres of radius a_s; (b) two disks of radius a_d, oriented face-to-face; and (c) two disks oriented side by side with an edge overlap distance z. The small purple spheres represent micelles (not to scale).

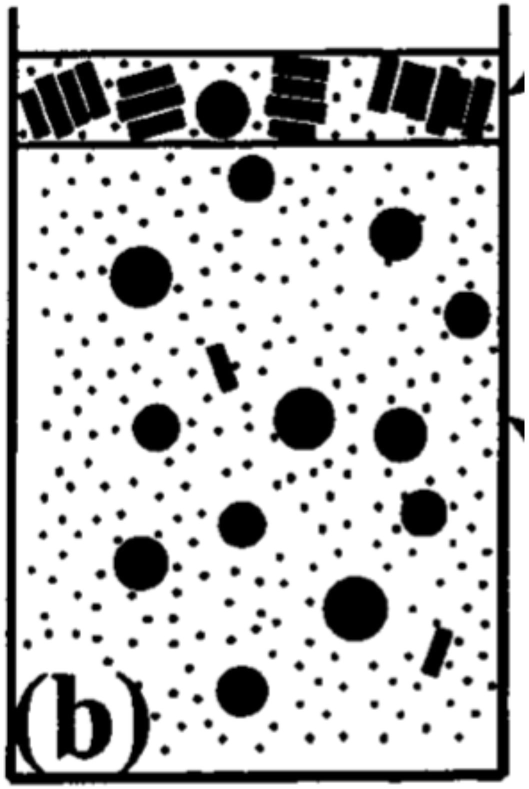

Another example

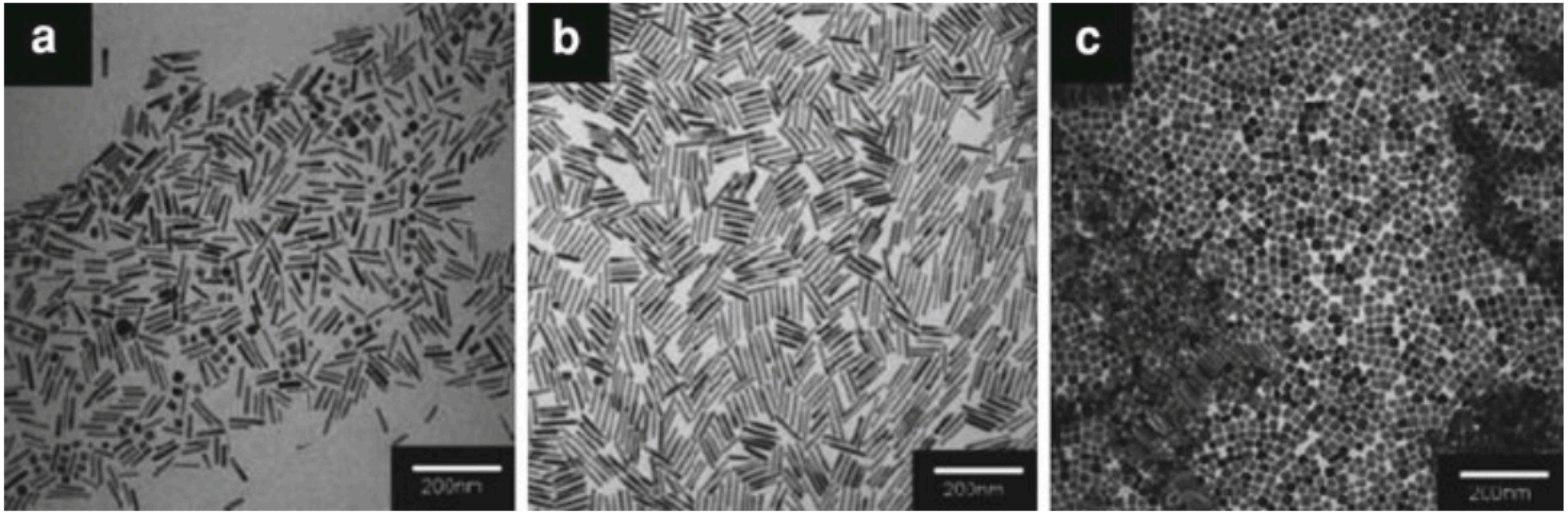

Fig. 1.29 TEM images of a dispersion of rod-like and cube-like gold colloids. **a** Synthesized mixture, **b** sediment, **c** supernatant. Picture reprinted from K. Park, H. Koerner, and R. A. Vaia, *Nano Lett.*, 10:1433, Copyright 2010, with permission from the American Chemical Society

Fig. 1.30 A large colloidal sphere near a step edge in a sea of small spheres. The presence of the small spheres lead to depletion zones (*light grey regions*) near the walls of the container and around the big sphere. Overlap of depletion zones is indicated by the *hatched area*. This overlap volume increases the volume accessible to the small spheres, thereby increasing their entropy

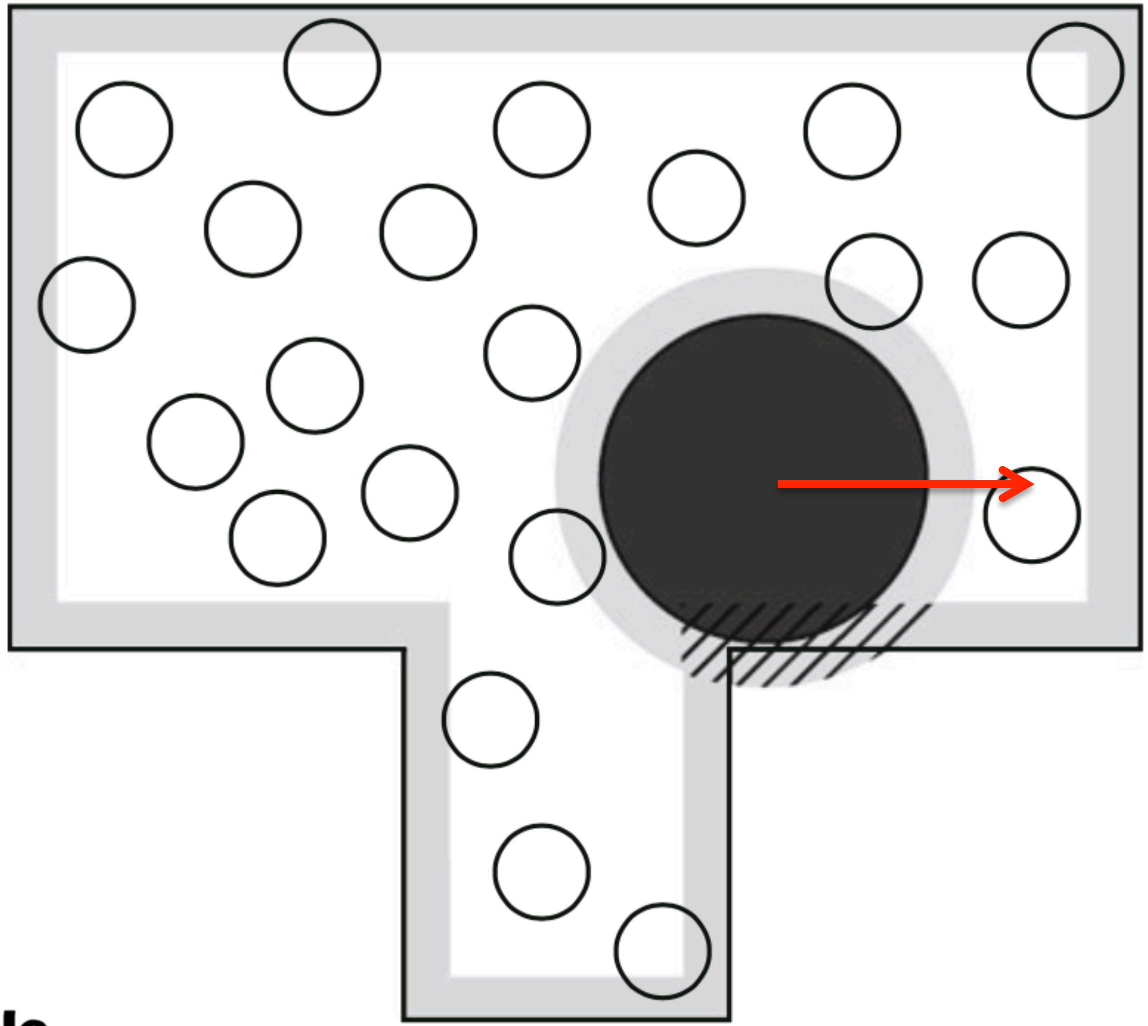

Entropic control of particle motion using passive surface microstructures

A. D. Dinsmore*, A. G. Yodh* & D. J. Pine†

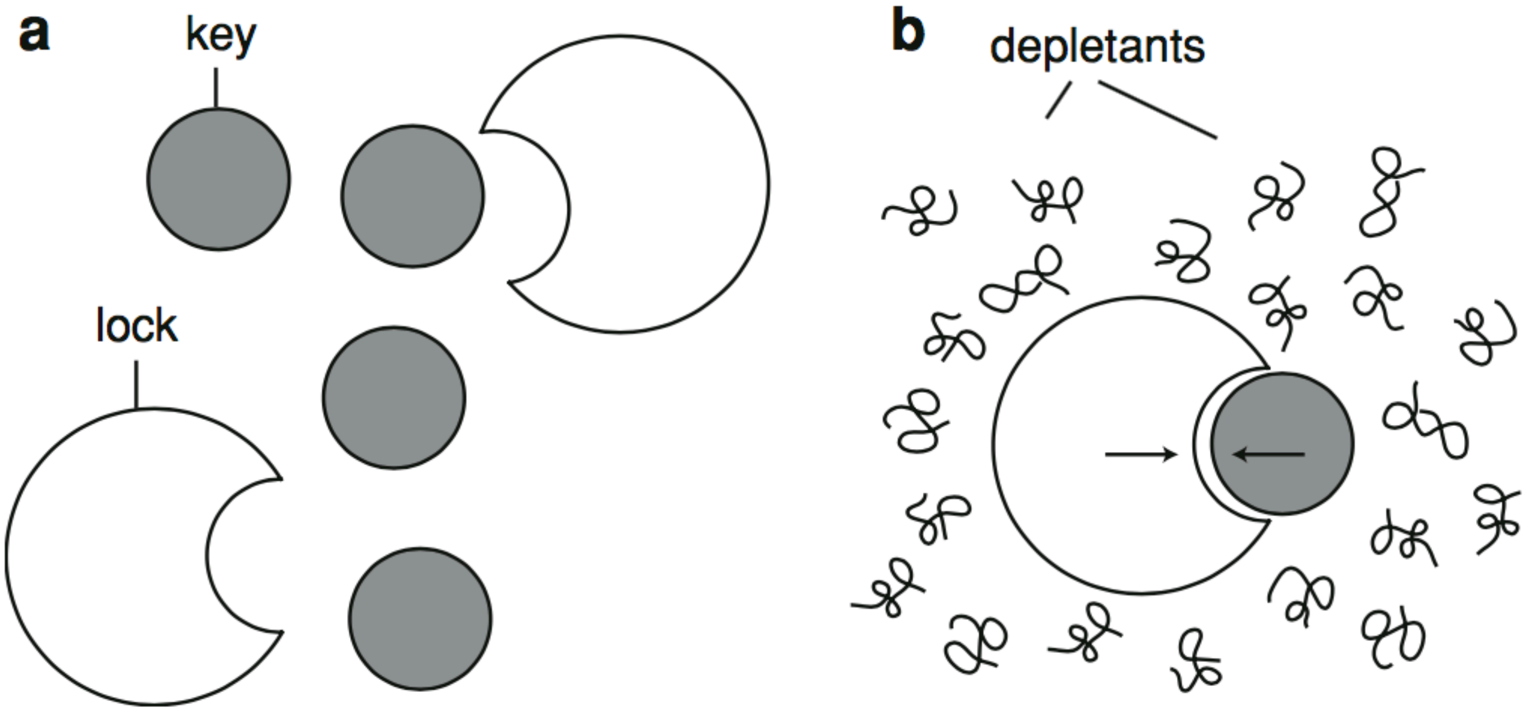

Fig. 1.31 **a** Colloidal ‘lock’ particles can be synthesized [284] containing a dimple into which ‘key’ particles, spherical colloids with appropriate size, can fit. **b** By adding depletants (polymer chains) a key can be pushed into a lock using the depletion force. Inspired by Solomon [285]

Lock and key colloids

S. Sacanna[1], W. T. M. Irvine[1], P. M. Chaikin[1] & D. J. Pine[1]

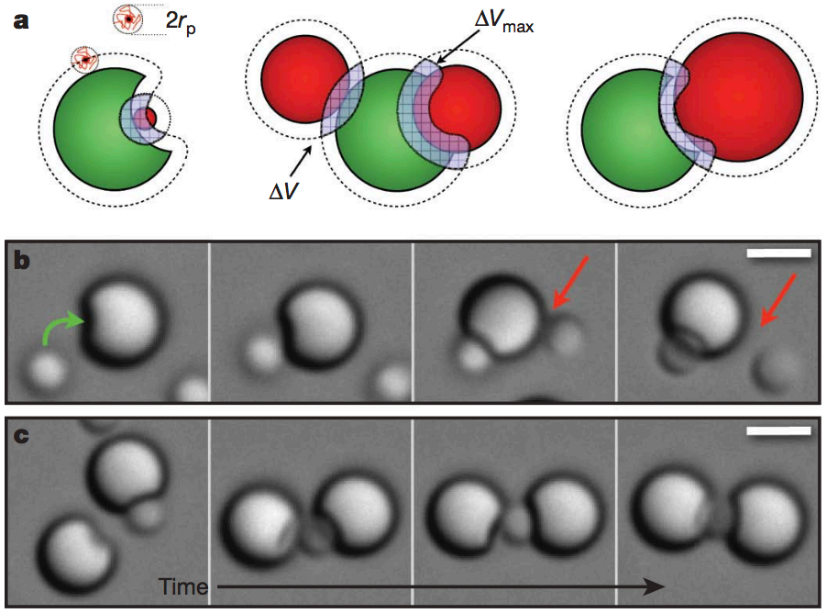

Figure 2 | Lock–key interactions. **a**, The depletion attraction potential between lock and key is proportional to the overlapping excluded volume ΔV, which attains a maximum ΔV_{max} for the configuration in which the key particle, by virtue of its size and position, precisely fits into the spherical cavity of a lock particle. For all other configurations, $\Delta V < \Delta V_{max}$. Because the depletion interaction is also proportional to the density n_p of the polymer depletant in solution, the interaction can be tuned by adjusting n_p so that it is sufficiently strong to bind two particles only for the lock-and-key configuration. **b**, **c**, Snapshots from a movie showing an example of depletion-driven self-assembly of lock and key particles. The site-specificity of the interactions is captured in sequence **b** in which arrows indicate examples of successful (green) and unsuccessful (red) lock–key binding. Scale bars, 2 μm.

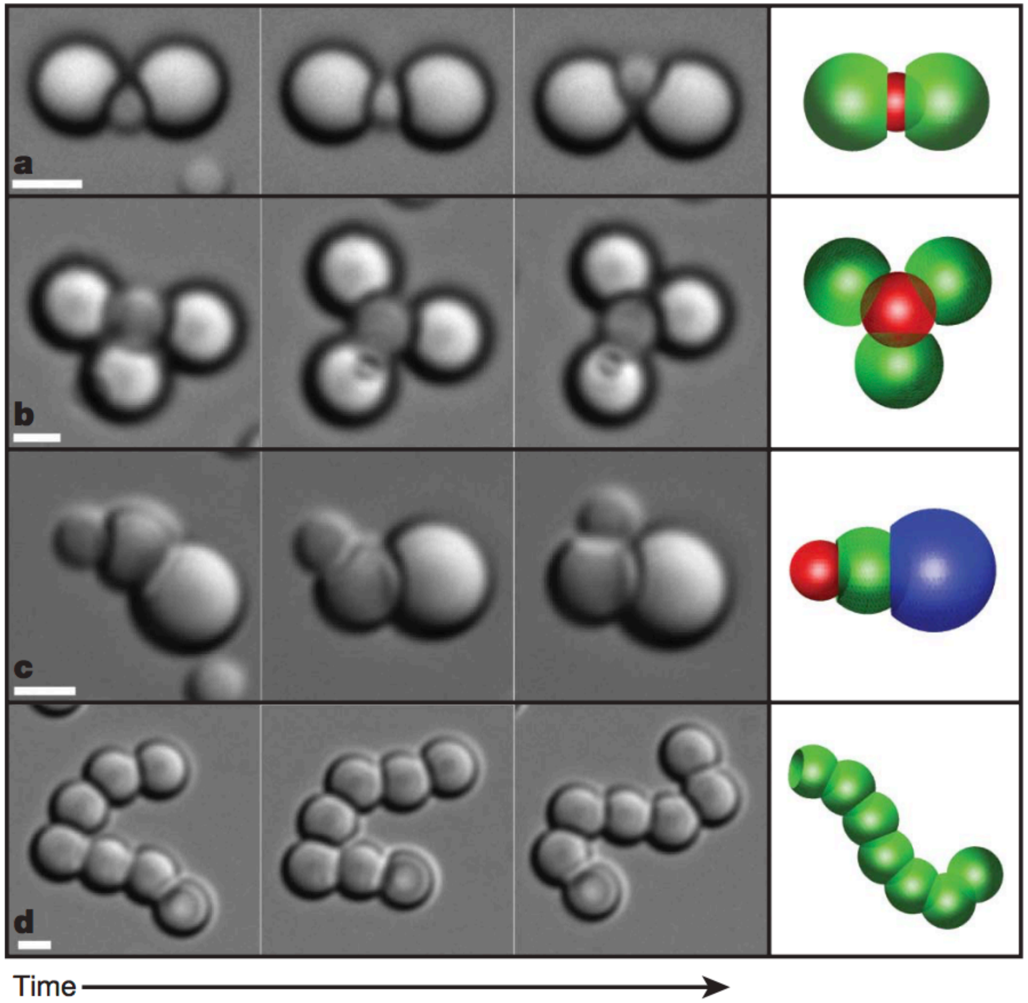

Figure 5 | Flexibility of the lock–key junctions in self-assembled colloidal molecules and polymers. Time-lapse optical microscopy images (left three columns), and schematics (rightmost column), show the flexibility of lock–key bonds in various assemblies (**a**–**d**), which are confined to two dimensions by being placed on a glass microscope slide. The absence of irreversible chemical bonds between the building blocks allows these ball-in-socket joints to move freely. Scale bars, 2 μm.

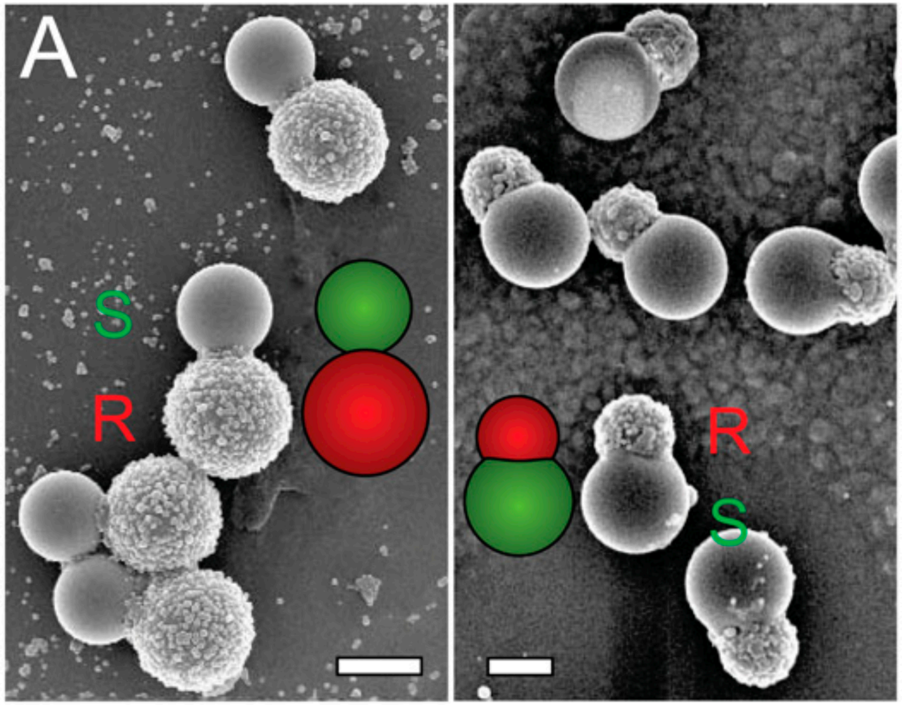

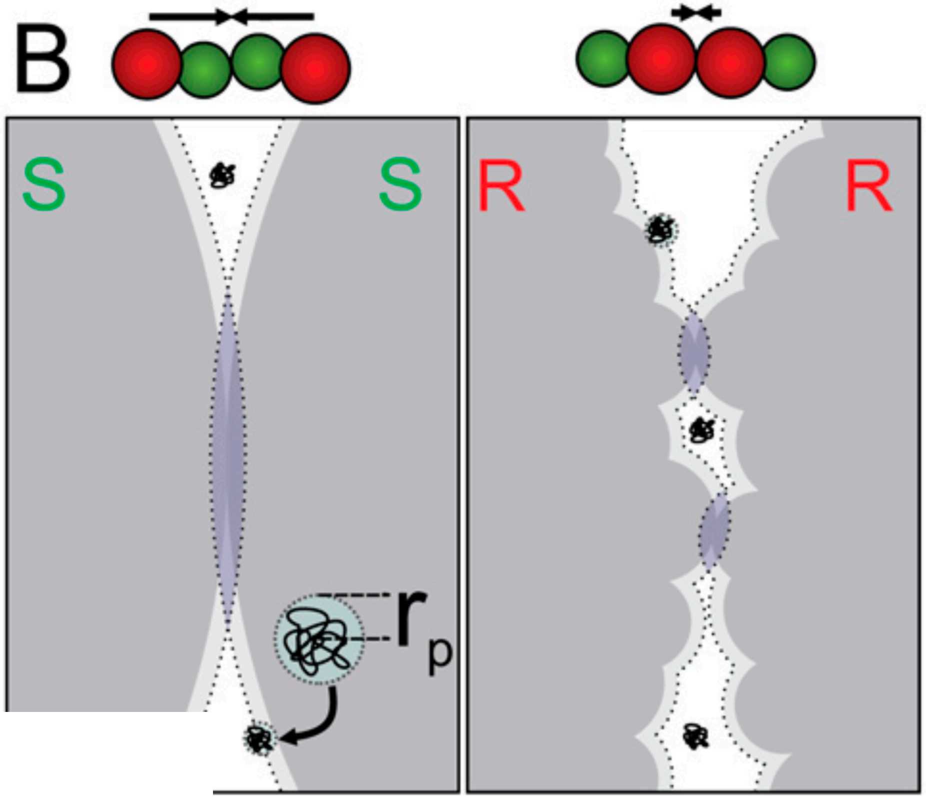

Surface roughness directed self-assembly of patchy particles into colloidal micelles

Daniela J. Kraft[a,1], Ran Ni[b], Frank Smallenburg[b], Michiel Hermes[b], Kisun Yoon[c], David A. Weitz[c], Alfons van Blaaderen[b],
Jan Groenewold[a], Marjolein Dijkstra[b], and Willem K. Kegel[a]

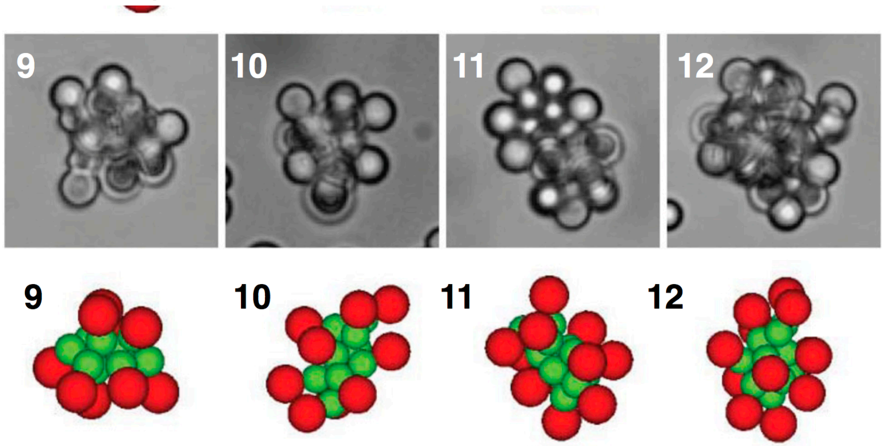

Playing with the properties of the co-solute

Depletant Shape...

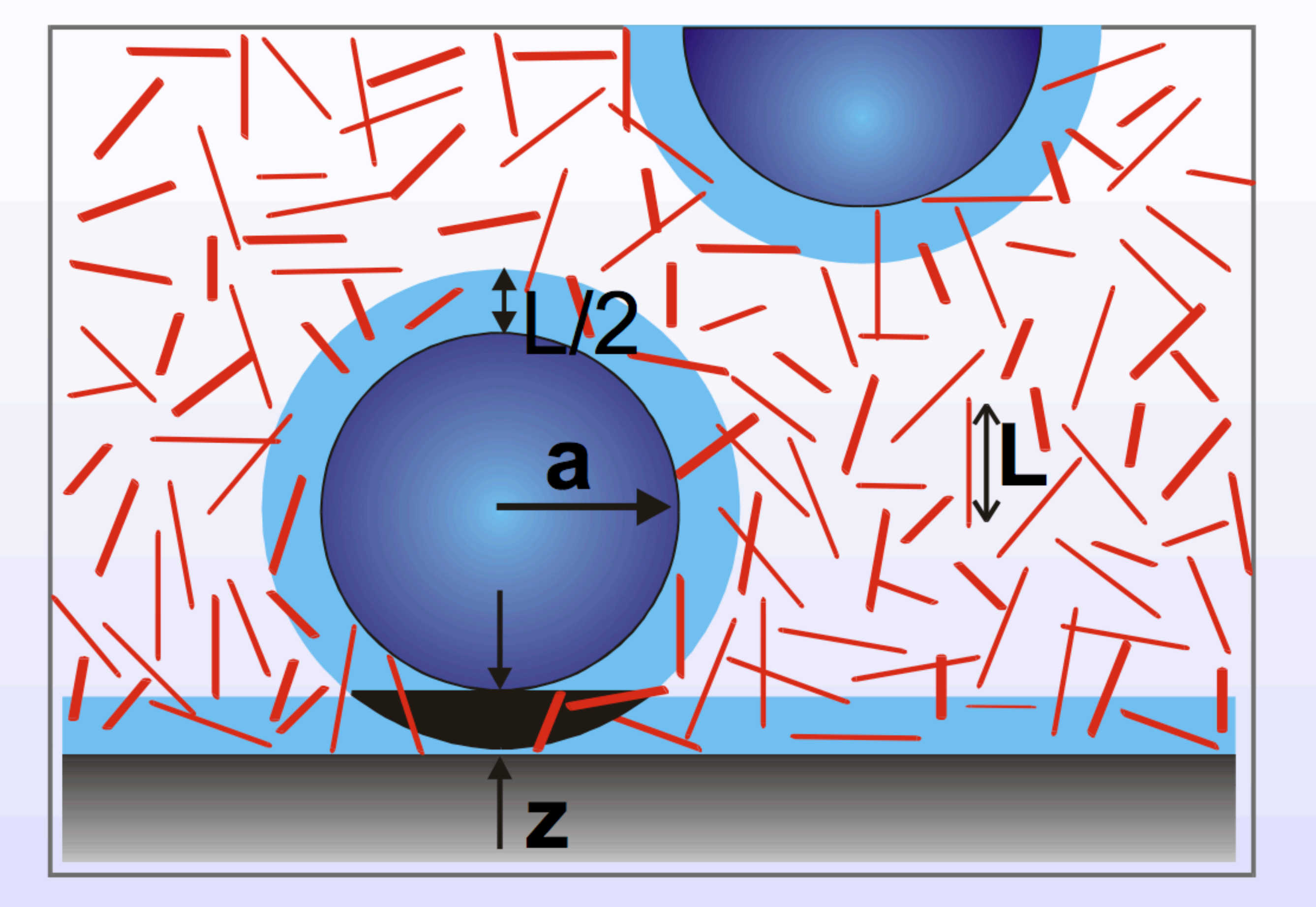

Polymerizing solvent ...

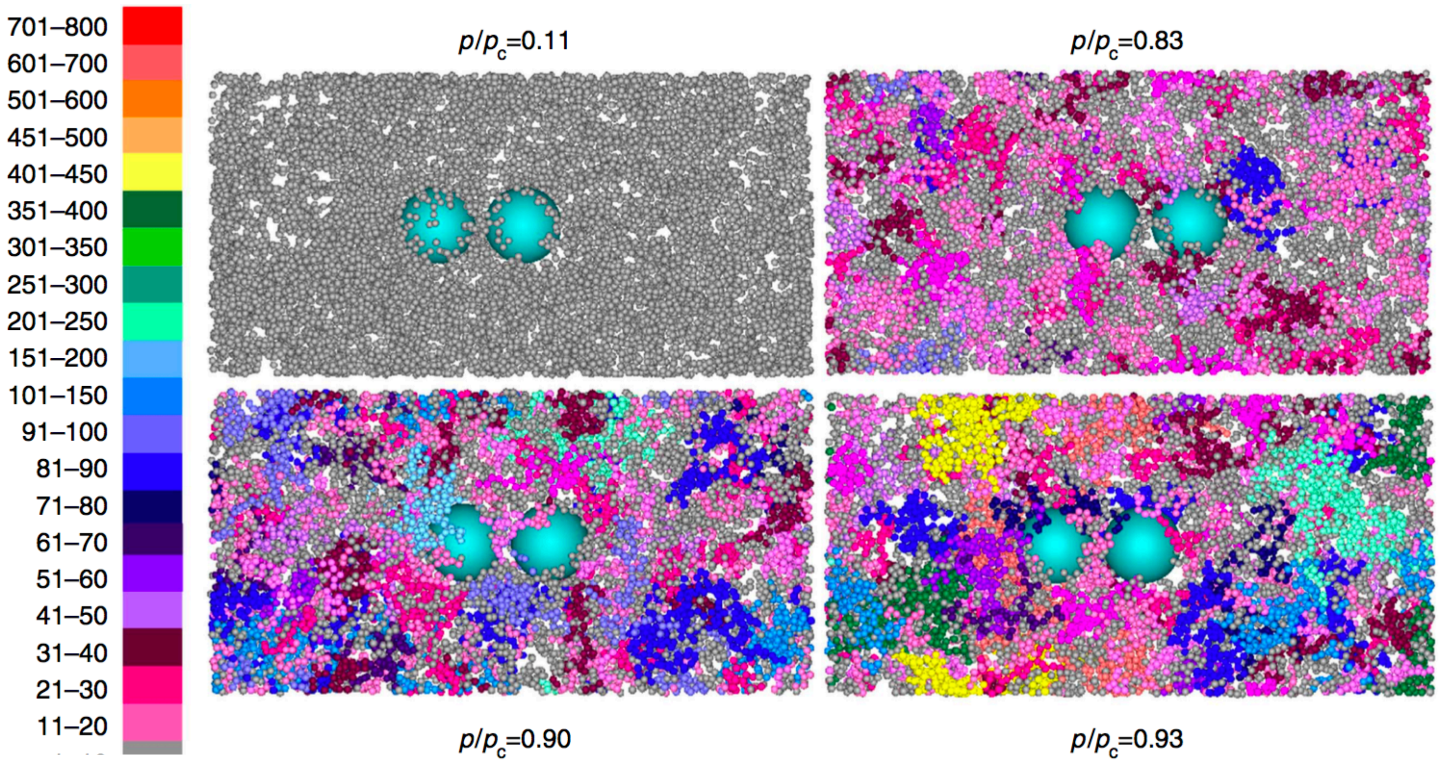

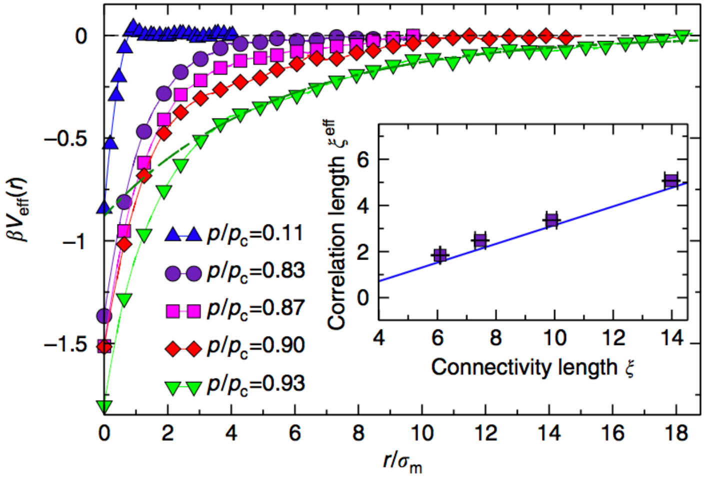

Figure 2 | Effective potentials between two colloids in a sol of clusters.

N. Gnan E. Zaccarellii and FS

DOI: 10.1038/ncomms4267